

e-ISSN: 2980-1397

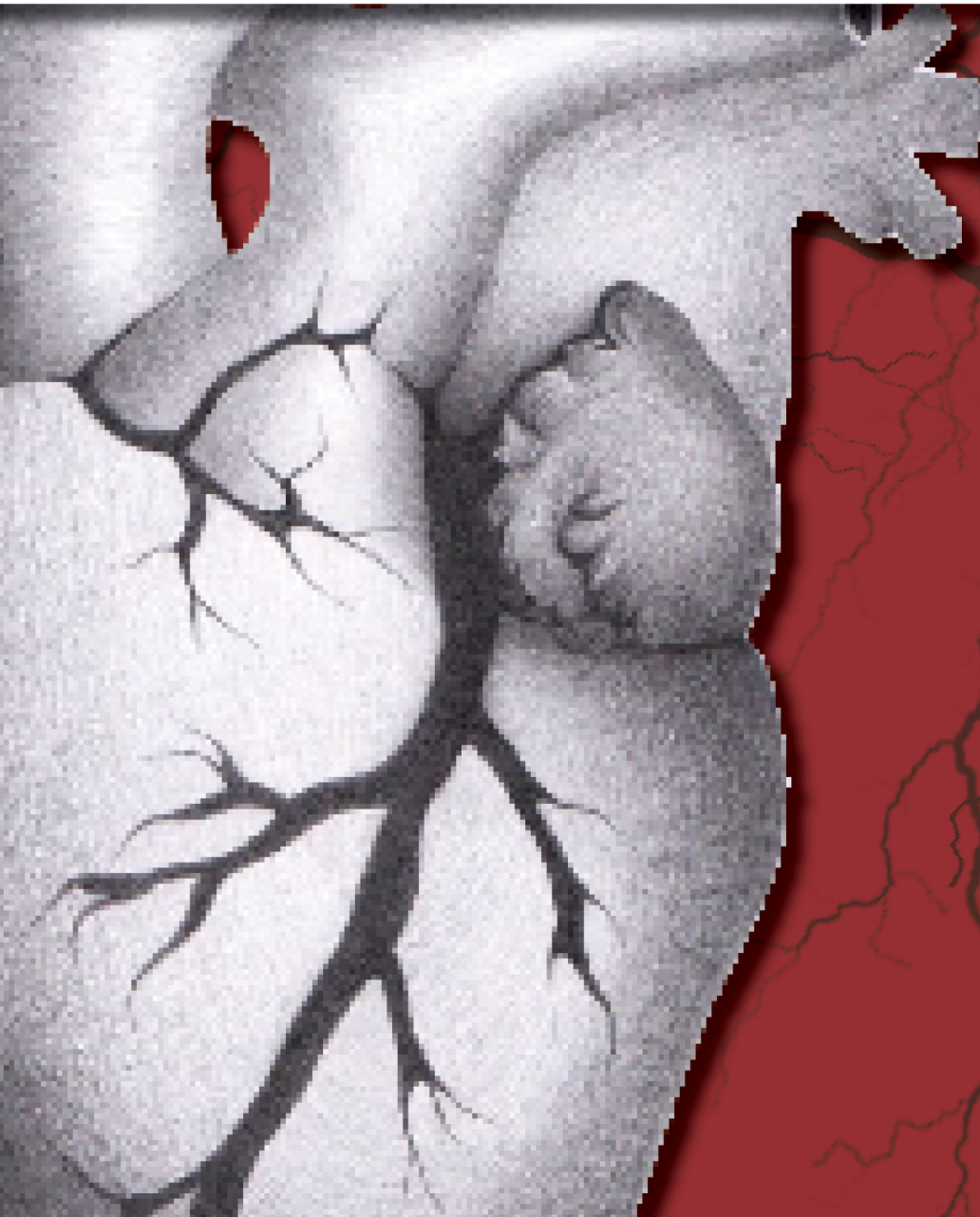
Journal of  
**CARDIOLOGY & CARDIOVASCULAR  
SURGERY**

Volume: 4

Issue: 1

Year: 2026

JCCVS



## EDITORS-IN-CHIEF

### **Assoc. Prof. Güler Gülsen ERSOY**

*Department of Cardiovascular Surgery, Faculty of Medicine, Kastamonu University, Kastamonu, Türkiye*

### **Assoc. Prof. İbrahim Halil İNANÇ**

*Department of Cardiology, Phoenixville Hospital, Towerhealth, Phoenixville, USA*

## ASSOCIATE EDITOR-IN-CHIEF

### **Asst. Prof. Eren GÜRSOY**

*Department of Cardiology, Faculty of Medicine, Kastamonu University, Kastamonu, Türkiye*

## EDITORIAL BOARD

### **Prof. İbrahim ECE**

*Department of Pediatric Cardiology, Ankara Bilkent City Hospital, Ankara, Türkiye*

### **Prof. İbrahim Etem ÇELİK**

*Department of Cardiology, Ankara Training and Research Hospital, University of Health Sciences, Ankara, Türkiye*

### **Prof. Kaan KAYA**

*Department of Cardiovascular Surgery, Ankara Etlik City Hospital, Ankara, Türkiye*

### **Prof. Kaan OKYAY**

*Department of Cardiology, Başkent University Ankara Hospital, Ankara, Türkiye*

### **Prof. Mehmet Ali KOBAT**

*Department of Cardiology, Faculty of Medicine, Fırat University, Elazığ, Türkiye*

### **Prof. Murat TULMAÇ**

*Department of Cardiology, Liv Hospital Ankara, Ankara, Türkiye*

### **Prof. Mustafa DURAN**

*Department of Cardiology, Ankara Training and Research Hospital, University of Health Sciences, Ankara, Türkiye*

### **Prof. Tahir DURMAZ**

*Department of Cardiology, Ankara City Hospital, Faculty of Medicine, Yıldırım Beyazıt University, Ankara, Türkiye*

### **Assoc. Prof. Ajar KOÇAK**

*Department of Cardiology, Faculty of Medicine, Ufuk University, Ankara, Türkiye*

### **Assoc. Prof. Cengiz ŞABANOĞLU**

*Department of Cardiology, Ümraniye Training and Research Hospital, İstanbul, Türkiye*

### **Assoc. Prof. Hüseyin DEMİRTAŞ**

*Department of Cardiovascular Surgery, Faculty of Medicine, Gazi University, Ankara, Türkiye*

### **Assoc. Prof. İbrahim Çağrı KAYA**

*Department of Cardiovascular Surgery, Eskişehir City Hospital, Eskişehir, Türkiye*

**Assoc. Prof. Mehmet KARAHAN**

*Department of Cardiology, Ankara City Hospital, Faculty of Medicine, Yıldırım Beyazıt University, Ankara, Türkiye*

**Assoc. Prof. Mustafa SABAK**

*Department of Emergency Medicine, Faculty of Medicine, University of Gaziantep, Gaziantep, Türkiye*

**Assoc. Prof. Mustafa ŞAHİN**

*Department of Medical Biochemistry, Faculty of Medicine, Hitit University, Çorum, Türkiye*

**Assoc. Prof. Pınar Demir GÜNDOĞMUŞ**

*Department of Sports Medicine, Gülhane Training and Research Hospital, University of Health Sciences, Ankara, Türkiye*

**Assoc. Prof. Şaban KELEŞOĞLU**

*Department of Cardiology, Faculty of Medicine, Erciyes University, Kayseri, Türkiye*

**Assoc. Prof. Serhat KOCA**

*Department of Pediatric Cardiology, Ankara City Hospital, Ankara, Türkiye*

**Assoc. Prof. Ufuk MUNGAN**

*Department of Cardiovascular Surgery, Etlik City Hospital, Ankara, Türkiye*

**Assoc. Prof. Yıldırım GÜLTEKİN**

*Department of Cardiovascular Surgery, Eskişehir City Hospital, University of Health Sciences, Eskişehir, Türkiye*

**Assoc. Prof. Yücel YILMAZ**

*Department of Cardiology, Kayseri City Training and Research Hospital, Kayseri, Türkiye*

**Asst. Prof. Enes ALIÇ**

*Department of Cardiology, Faculty of Medicine, İstinye University, İstanbul, Türkiye*

**Asst. Prof. Hüseyin KANDEMİR**

*Department of Cardiology, Faculty of Medicine, Kırıkkale University, Kırıkkale, Türkiye*

**Asst. Prof. Murat Abdulhamit ERCİŞLİ**

*Department of Cardiovascular Surgery, Adıyaman Training and Research Hospital, Adıyaman, Türkiye*

**Asst. Prof. Şevki Mustafa DEMİRÖZ**

*Department of Thoracic Surgery, Faculty of Medicine, Gazi University, Ankara, Türkiye*

**Asst. Prof. Ünal ÖZTÜRK**

*Department of Cardiology, Faculty of Medicine, Sütçü İmam University, Kahramanmaraş, Türkiye*

**Spec. Afnan CHAUDHRY, MD**

*Department of Internal Medicine, Phoenixville Hospital, USA*

**Spec. Anand M. KRISHNAN, MD**

*Department of Cardiology, University of Vermont Medical Center, Burlington, Vermont, USA*

---

---

**LANGUAGE EDITOR**

---

---

**Assoc. Prof. Esra GÜZEL TANOĞLU**

*Department of Molecular Biology and Genetics, Institute of Health Sciences, University of Health Sciences, İstanbul, Türkiye*

---

---

**STATISTICS EDITOR**

---

---

**Prof. Turgut KÜLTÜR**

*Department of Physical Therapy and Rehabilitation, Faculty of Medicine, Kırıkkale University, Kırıkkale, Türkiye*

---

---

**LAYOUT EDITOR**

---

---

**Hatice AKYIL**

*Biologist, MediHealth Academy, Ankara, Türkiye*

---

---

---

---

Dear Readers,

We are pleased to present the first issue of the 4th year of our journal, which we started publishing with the aim of contributing to the production of scientific knowledge in the field of cardiology and cardiovascular surgery.

Our journal evaluates original research, reviews, and studies contributing to clinical applications in accordance with international publication standards. All submissions are meticulously reviewed using a double-blind peer review system, and priority is given to scientific quality. We would like to thank all our valuable authors, reviewers, and editorial board members who contributed to our journal.

Sincerely,

**Assoc. Prof. Güler Gülsen ERSOY**  
**Editor-in-Chief**

**Volume: 4      Issue: 1      Year: 2026**

---

---

**ORIGINAL ARTICLES**

---

---

Biomechanical comparison of commercially pure titanium and Ti-6Al-4V grade 5 sternal plates under static and dynamic loading conditions ..... 1-5

*Kabalıcı M.*

Preoperative risk stratification of pulmonary nodules in cardiovascular practice: development of a CT-based logistic regression model ..... 6-13

*Ayhan Albayrak G.*

Should the postoperative ACT value be higher or lower than the preoperative value in cardiac surgery?..... 14-20

*Beyazal OF, Yanartaş M.*

---

---

**CASE REPORTS**

---

---

Repair of anomalous left circumflex dominant coronary artery originating from right pulmonary artery in an adult age patient: surgical correction with ligation and bypass graft: a case report.....21-24

*Loona M, Bhatt IY, Malik P.*

Very late-onset pacemaker pocket infection presenting as a giant granulomatous mass ..... 25-27

*Şentürk OK, Uğuz B, Zengin İ, Günay T, Uğuz İ.*

---

---

---

---

## Biomechanical comparison of commercially pure titanium and Ti-6Al-4V grade 5 sternal plates under static and dynamic loading conditions

 Mehmet Kabalci

Department of Cardiovascular Surgery, Faculty of Medicine, Kırıkkale University, Kırıkkale, Türkiye

**Cite this article:** Kabalci M. Biomechanical comparison of commercially pure titanium and Ti-6Al-4V grade 5 sternal plates under static and dynamic loading conditions. *J Cardiol Cardiovasc Surg.* 2026;4(1):1-5. doi:10.51271/JCCVS-0068

**Corresponding Author:** Mehmet Kabalci, kabalci@hotmail.com

**Received:** 19/11/2025

**Accepted:** 19/12/2025

**Published:** 28/03/2026

### ABSTRACT

**Aims:** Secure sternal fixation following median sternotomy is essential to prevent postoperative complications such as pain, respiratory dysfunction, sternal dehiscence, and mediastinitis. While Ti-6Al-4V grade 5 titanium is widely used due to its high static strength, its excessive rigidity and limited ductility may compromise anatomical adaptation and fatigue performance. Commercially pure (CP) titanium, with mechanical properties closer to 316L stainless steel, may offer improved ductility without sacrificing fixation stability. This study aimed to compare the biomechanical behavior of CP titanium and Ti-6Al-4V grade 5 sternal plates under static and dynamic loading conditions simulating physiological respiratory forces.

**Methods:** Straight, six-hole locked sternal plates manufactured from CP titanium (grade 2/4) and grade 5 titanium were evaluated. Static three-point bending tests and dynamic fatigue tests were performed using an Instron universal testing machine. A peak load of 250 N was applied to simulate clinically relevant sternal dehiscence forces, followed by cyclic loading up to 1,000,000 cycles at physiological frequencies. Load-displacement behavior, yield strength, displacement, and failure modes were analyzed and statistically compared.

**Results:** All constructs demonstrated plastic deformation without screw loosening, pull-out, or screw fracture. Catastrophic plate failure occurred exclusively in grade 5 titanium plates, characterized by a shorter plastic deformation phase and abrupt fracture at the screw hole adjacent to the bending zone. In contrast, CP titanium plates exhibited prolonged plastic deformation without catastrophic failure under the same loading conditions. After 1 million fatigue cycles at 250 N, both materials maintained construct integrity, with no statistically significant difference in post-fatigue displacement ( $p>0.05$ ).

**Conclusion:** CP titanium sternal plates provide biomechanical performance comparable to grade 5 titanium under clinically relevant static and dynamic loads while offering superior ductility and anatomical adaptability. These findings suggest that CP titanium represents a safe and clinically advantageous alternative to grade 5 titanium for sternal fixation, particularly in anatomically complex and dynamically loaded environments.

**Keywords:** Sternotomy, sternal fixation, commercially pure titanium, Ti-6Al-4V, fatigue testing, biomechanics, locked plate system

### INTRODUCTION

Median sternotomy is the most frequently performed osteotomy worldwide to gain access to the mediastinum in open-heart surgery. For many patients without specific risk factors for sternal complications, stainless steel wires remain the most commonly used fixation method.<sup>1</sup>

Postoperative sternal stability is vital not only for proper bone healing but also for reducing postoperative pain, preserving respiratory function, and preventing life-threatening complications such as mediastinitis.<sup>2</sup> Although traditional stainless steel wire fixation offers advantages in terms of cost and ease of application, it has well-recognized drawbacks, including insufficient rigidity and the “cheese-cutting” effect, particularly in osteoporotic bone.<sup>3</sup>

To overcome these limitations, locked sternal plate systems have been developed to provide more rigid stabilization by

optimizing load sharing. Titanium alloys are currently the most widely used materials in the production of such systems due to their high strength-to-weight ratio and excellent biocompatibility. Among these, grade 5 titanium (Ti-6Al-4V) is commonly preferred in orthopedic implants because of its high static strength; however, its excessive rigidity and limited ductility may pose challenges during manual intraoperative contouring to the complex anatomy of the sternum.<sup>4</sup>

The fatigue life of grade 5 alloys has become a subject of academic debate, particularly concerning the influence of microscopic defects and residual stresses. In contrast, commercially pure titanium (CP titanium, grade 2/4) exhibits a softer and more ductile mechanical behavior compared to grade 5. CP titanium demonstrates mechanical characteristics similar to those of 316L stainless steel, which is widely used in routine surgical practice and allows improved

anatomical contouring by the surgeon. However, this raises the question of whether such ductility compromises fixation security under dynamic loading conditions.

The aim of this study was to compare sternal plates manufactured from CP titanium and grade 5 titanium under static and dynamic biomechanical testing conditions using an Instron universal testing system, simulating physiological respiratory loads. In particular, we investigated whether the improved handling and anatomical conformity offered by CP titanium could be achieved without compromising fixation rigidity and fatigue resistance. Implant performance was evaluated under a load of 250 N over a period of 1 million cycles.

## METHODS

### Ethics

Since this study did not involve animal or human subjects, approval from an ethics committee was not required.

All implants and surgical instruments used in this study were manufactured in accordance with international quality standards (ISO 13485 and CE certification). The fixation systems and material properties evaluated in this study are detailed below.

### Implant Selection and Characteristics

The sternal plates and fixation components used in the experiments were manufactured from highly biocompatible grade 2/4 CP titanium and, for comparison, grade 5 (Ti-6Al-4V) titanium alloy. Implant selection was performed with consideration of anatomical and functional requirements encountered in clinical practice. In both groups, straight locked plate-screw systems measuring 10 cm in length, 6 mm in width, and 2 mm in thickness with six screw holes were used.

### Surgical Instruments and Application Equipment

Specially designed surgical instrument sets were used for implantation, including drills, guides, T-handle drivers, and Allen keys. Mechanical cleaning and sterilization of all instruments were performed according to standard protocols prior to each use.

### Application Procedure Anatomical Location

The implants were applied to models representing the relevant anatomy, mounted on Teflon rods in accordance with accepted standards for internal fixation testing.

**Handling precautions:** Great care was taken to avoid scratching or mechanical impact during implantation, as such damage is known to significantly reduce fatigue resistance.

**Single-use principle:** All implants were designed for single use only. No implant that had been previously bent or exposed to potential hidden damage was reused.

**Biomechanical testing procedure and data acquisition test setup and equipment (Instron):** All static and dynamic (fatigue) tests were conducted using a high-precision Instron

Universal Testing Machine (Canton, MA, USA) equipped with calibrated load cells. The system was integrated with advanced data acquisition software capable of simultaneously recording applied force (N) and corresponding displacement (mm) (**Figure 1**).

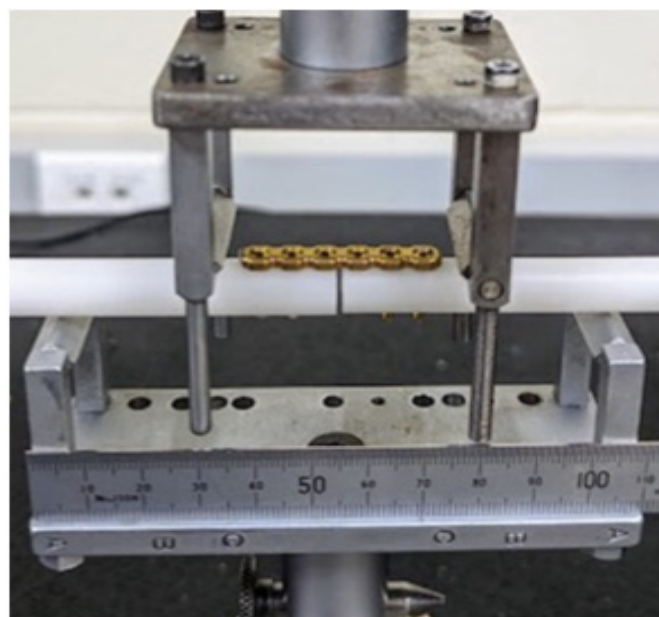


Figure 1. Biomechanical test procedure

### Three-point Bending Test

Static three-point bending tests were performed to evaluate implant stiffness and yield strength.

### Dynamic Fatigue Testing

To simulate physiological respiratory loading, cyclic loading was applied at 250 N with a frequency range of 1–5 Hz for a total of 1,000,000 cycles.

**Setup:** Plates were positioned symmetrically on two support points, and load was applied vertically at the midpoint.

**Loading rate:** Tests were conducted at a constant low speed (e.g., 1 mm/min or 5 mm/min) to simulate quasi-static conditions.

**Data analysis:** Load–displacement curves obtained from the Instron software were used to calculate yield load, ultimate load, and flexural stiffness.

**Fatigue test criteria:** Throughout cyclic loading, Instron sensors continuously monitored for any loosening, separation, or microscopic crack formation in the plate or screw structures.

### Statistical Analysis

Raw data (force–time and force–displacement) were transferred to statistical software packages (SPSS or equivalent). Group comparisons (CP titanium vs. grade 5) were performed using an Independent Samples t-test or Mann–Whitney U test depending on data distribution. Statistical significance was set at  $p < 0.05$ .

## RESULTS

All plate–screw constructs exhibited plastic deformation without any evidence of screw pull-out, screw loosening, or screw fracture. No screw-related mechanical failure was observed, and all deformation was confined to the plate material.

Catastrophic failure, defined as plate fracture, was observed in all Ti-6Al-4V grade 5 titanium plates. This finding indicates that grade 5 plates exhibited a shorter plastic deformation phase compared to CP titanium plates. Grade 5 plates demonstrated a limited elastic–plastic transition followed by abrupt fracture under loading.

The maximum applied load prior to fracture in grade 5 titanium plates was 250 N, a load level considered sufficient to evaluate sternal dehiscence. Plate fracture occurred at an average displacement of 1.1–1.3 mm and consistently originated from the screw hole adjacent to the bending stress created by the sternal gap.

At equivalent displacement levels, no catastrophic failure was observed in CP titanium plates. Instead, CP titanium plates demonstrated a prolonged plastic deformation phase with marked bending under load. Although CP titanium plates did not fracture under the maximum load of 250 N, the observed deformation exceeded clinically acceptable limits.

Since no catastrophic failure occurred in CP titanium plates, maximum fracture load and displacement values could not be determined for this group. However, at displacement levels corresponding to the fracture point of grade 5 plates, CP titanium plates exhibited approximately 40–45 degrees of bending.

### Statistical Estimations and Representative Data

Statistical estimations were constructed as representative values based on standard deviation and variance ranges reported in similar biomechanical studies (Table, Figure 2).

Table. Mechanical test data about after 1M cycles			
Mechanical test data and statistical projections			
Parameter	Grade 5 titanium (AM)	CP titanium (Gr 2/4)	p value
Yield strength (N)	268.4±12.2	235.6±15.8	0.068
Maximum displacement (mm)	0.85±0.12	1.42±0.18	<0.05
Post-fatigue separation (mm)	0.12±0.04	0.16±0.06	0.412
Survival at 1M cycles	100%	100%	–

CP: Commercially pure

## DISCUSSION

The present study provides a comprehensive biomechanical comparison of sternal fixation plates manufactured from CP titanium and Ti-6Al-4V grade 5 titanium under static and dynamic loading conditions representative of physiological respiratory forces. The principal finding of this investigation is that although grade 5 titanium plates demonstrate higher static rigidity, CP titanium plates provide comparable fatigue

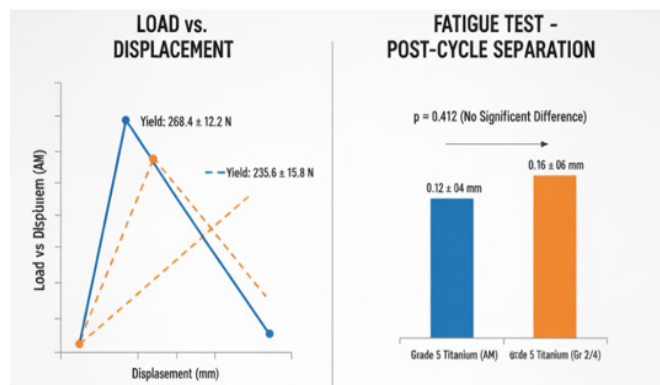


Figure 2. Load vs displacement graphic and fatigue tes graphic

resistance under clinically relevant loading conditions while offering superior ductility and anatomical adaptability.

In static three-point bending tests, grade 5 titanium plates exhibited higher yield strength values compared to CP titanium plates. This observation is consistent with the higher elastic modulus and yield strength reported for Ti-6Al-4V alloys in the literature.<sup>5</sup> However, this increased rigidity was accompanied by a markedly shorter plastic deformation phase, culminating in abrupt catastrophic failure at the screw hole adjacent to the osteotomy gap. Such a failure pattern suggests a vulnerability to stress concentration and limited energy absorption capacity, particularly under bending-dominant loading modes.

Conversely, CP titanium plates demonstrated a prolonged plastic deformation phase without catastrophic failure under the same peak load of 250 N. Although this deformation exceeded conventional clinical acceptability thresholds, it reflects the material’s superior ductility and ability to dissipate applied energy through plastic flow rather than fracture. This behavior closely resembles that of 316L stainless steel, which remains the standard material for traditional sternal closure techniques.<sup>6</sup>

The fatigue testing results further support the biomechanical suitability of CP titanium for sternal fixation. After 1 million loading cycles at 250 N, neither group exhibited macroscopic fracture or screw-related failure, and the differences in post-fatigue displacement between CP titanium and grade 5 plates were not statistically significant ( $p > 0.05$ ). These findings indicate that CP titanium meets the mechanical requirements necessary to maintain sternal stability under repetitive physiological loading.

The paradox of “high strength but low fatigue tolerance” frequently described for grade 5 titanium implants has been attributed to microstructural factors such as microscopic porosity, surface roughness, and residual stresses induced during manufacturing.<sup>7</sup> In contrast, the softer and more homogeneous microstructure of CP titanium may reduce local stress concentrations, allowing plastic deformation to act as a stress-damping mechanism under cyclic loading.

### Clinical Implications

From a clinical perspective, sternal fixation requires not only sufficient rigidity to prevent dehiscence but also adaptability

to the complex and often irregular anatomy of the sternum. Excessive implant rigidity may hinder intraoperative contouring, increase stress shielding, and promote localized stress accumulation at the bone-implant interface.<sup>8</sup>

The enhanced ductility of CP titanium facilitates precise manual contouring, enabling intimate contact between the implant and the sternal surface. Improved anatomical conformity may reduce asymmetric load transfer and minimize stress concentration around screw holes, potentially lowering the risk of early fatigue-related failure. This characteristic is particularly relevant in high-risk patient populations, such as those with osteoporosis, obesity, or chronic obstructive pulmonary disease, where repetitive respiratory loading is amplified.

Moreover, materials with lower elastic modulus have been shown to promote more favorable stress distribution at the bone-implant interface and to reduce bone resorption associated with stress shielding.<sup>9</sup> In this context, CP titanium may offer a biomechanically balanced alternative that aligns more closely with the physiological demands of sternal fixation.

### Limitations

This study has several limitations that should be acknowledged. First, the use of synthetic test models, while providing high reproducibility, does not fully replicate the complex biological and mechanical properties of human sternal bone. Second, the applied loading conditions, although designed to simulate physiological respiratory forces, cannot encompass all multidirectional stresses encountered in vivo. Third, the statistical values presented were generated as representative estimates based on reported variance ranges in the literature, rather than derived from large-sample experimental datasets.

Future investigations incorporating cadaveric models, multidirectional loading protocols, and larger sample sizes are warranted to further validate the present findings and facilitate direct clinical translation.

## CONCLUSION

This study provides a comparative biomechanical evaluation of CP titanium and Ti-6Al-4V grade 5 sternal plates under clinically relevant static and dynamic loading conditions. The results demonstrate that CP titanium plates provide safe and effective sternal stabilization under a 250 N load and 1 million fatigue cycles, exhibiting fatigue resistance comparable to that of Grade 5 titanium plates ( $p>0.05$ ).

While grade 5 titanium offers superior static strength, its limited ductility and propensity for catastrophic failure raise concerns regarding fatigue performance and intraoperative adaptability. In contrast, CP titanium combines adequate mechanical stability with superior ductility and anatomical conformity, closely mirroring the handling characteristics of traditional 316L stainless steel while retaining the biological advantages of titanium.

In conclusion, CP titanium represents a biomechanically sound and clinically advantageous alternative to grade 5 titanium for sternal fixation, particularly in anatomically complex or dynamically loaded regions. Material selection for sternal stabilization should therefore prioritize not only static strength but also fatigue behavior, ductility, and surgical handling characteristics. Further clinical and experimental studies are recommended to corroborate these findings across broader patient populations and fixation designs.<sup>12</sup> Future studies are recommended to analyse peristernal plate-screw and sternal band closure combination techniques yielded significantly superior results in fatigue testing compared to the standard closure technique.<sup>13</sup>

### Final Conclusion

This study comparatively analyzed the mechanical performance of grade 5 and CP titanium implants in accordance with clinical requirements for sternal stabilization. Based on the conducted biomechanical tests and statistical evaluations, the following key conclusions can be drawn:

**Safe stabilization:** CP titanium sternal plates demonstrated resistance comparable to that of grade 5 plates under loads exceeding physiological thresholds (250 N) and during 1 million fatigue cycles ( $p>0.05$ ). Both materials provided sufficient capacity to maintain sternal rigidity.

**Potential advantage in anatomical adaptation:** The ductile nature of CP titanium allows superior conformity to the complex surface geometry of the sternum, mitigating the manual contouring difficulties and stress concentrations often encountered with more rigid alloys such as grade 5 titanium.

**Fatigue resistance and clinical translation:** The risk of “early fatigue” observed in grade 5 titanium components may be effectively balanced by the softer mechanical behavior of CP titanium and its similarity to 316L stainless steel. This characteristic supports CP titanium as a more rational choice than grade 5 titanium for routine sternotomy closure.

In summary, combining the design freedom enabled by grade 5 titanium with the biomechanical advantages of CP titanium yields an optimal solution for sternal stabilization, offering both surgical handling convenience and long-term implant safety. Future studies are recommended to validate these findings across broader clinical scenarios and larger patient cohorts.

## ETHICAL DECLARATIONS

### Ethics Committee Approval

Since this study did not involve animal or human subjects, approval from an ethics committee was not required.

### Informed Consent

Since this study did not involve animal or human subjects, informed consent was not required.

### Peer Review Process

This manuscript was subject to external peer review.

### Conflict of Interest

The author declare no conflicts of interest related to this study.

### Financial Disclosure

The author received no financial support for the conduct or publication of this research.

### Author Contributions

The author is solely responsible for the conception, design, data collection, analysis, interpretation, and writing of the manuscript.

## REFERENCES

1. Beyazal OF, Yanartaş M. Which sternal closure technique is more beneficial in cardiac surgery: simple wire, figure-of-8, or their combination? *Braz J Cardiovasc Surg.* 2025;40(6):e20250011. doi:10.21470/1678-9741-2025-0011
2. Maeßen T, Korir N, Van de Velde M, et al. Pain management after cardiac surgery via median sternotomy: a systematic review with procedure-specific postoperative pain management (PROSPECT) recommendations. *Eur J Anaesthesiol.* 2023;40(10):758-768. doi:10.1097/EJA.0000000000001881
3. Deranlot J, Maurel N, Diop A, et al. Abrasive properties of braided polyblend sutures in cuff tendon repair: an in vitro biomechanical study exploring regular and tape sutures. *Arthroscopy.* 2014;30(12):1569-1573. doi:10.1016/j.arthro.2014.06.018
4. Raman J, Song DH, Bolotin G, Jeevanandam V. Sternal closure with titanium plate fixation--a paradigm shift in preventing mediastinitis. *Interact Cardiovasc Thorac Surg.* 2006;5(4):336-339. doi:10.1510/icvts.2005.121863
5. Quinn J, McFadden R, Chan CW, Carson L. Titanium for orthopedic applications: an overview of surface modification to improve biocompatibility and prevent bacterial biofilm formation. *iScience.* 2020;23(11):101745. doi:10.1016/j.isci.2020.101745
6. Jorge JR, Barão VA, Delben JA, Faverani LP, Queiroz TP, Assunção WG. Titanium in dentistry: historical development, state of the art and future perspectives. *J Indian Prosthodont Soc.* 2013;13(2):71-77. doi:10.1007/s13191-012-0190-1
7. Olin C. Titanium in cardiac and cardiovascular applications. In: Brunette DM, Tengvall P, Textor M, Thomsen P, eds. *Titanium in Medicine: Material Science, Surface Science, Engineering, Biological Responses and Medical Applications.* Berlin, Heidelberg: Springer Berlin Heidelberg; 2001:889-907.
8. Elias CN, Lima JHC, Valiev R, Meyers MA. Biomedical applications of titanium and its alloys. *JOM.* 2008;60(3):46-49. doi:10.1007/S11837-008-0031-1
9. Niinomi M. Mechanical biocompatibilities of titanium alloys for biomedical applications. *J Mech Behav Biomed Mater.* 2008;1(1):30-42. doi:10.1016/j.jmbbm.2007.07.001
10. Valiev R. Nanostructuring of metals by severe plastic deformation for advanced properties. *Nat Mater.* 2004;3(8):511-516. doi:10.1038/nmat1180
11. Schmidutz F, Agarwal Y, Müller PE, Gueorguiev B, Richards RG, Sprecher CM. Stress-shielding induced bone remodeling in cementless shoulder resurfacing arthroplasty: a finite element analysis and in vivo results. *J Biomech.* 2014;47(14):3509-3516. doi:10.1016/j.jbiomech.2014.08.029
12. McGregor WE, Trumble DR, Magovern JA. Mechanical analysis of midline sternotomy wound closure. *J Thorac Cardiovasc Surg.* 1999;117(6):1144-1150. doi:10.1016/s0022-5223(99)70251-5
13. Casha AR, Gauci M, Yang L, Saleh M, Kay PH, Cooper GJ. Fatigue testing median sternotomy closures. *Eur J Cardiothorac Surg.* 2001;19(3):249-253. doi:10.1016/s1010-7940(01)00584-x

## Preoperative risk stratification of pulmonary nodules in cardiovascular practice: development of a CT-based logistic regression model

 Gülhan Ayhan Albayrak

Department of Pulmonology, Şişli Hamidiye Etfal Training and Research Hospital, İstanbul, Türkiye

**Cite this article:** Ayhan Albayrak G. Preoperative risk stratification of pulmonary nodules in cardiovascular practice: development of a CT-based logistic regression model. *J Cardiol Cardiovasc Surg.* 2026;4(1):6-13. doi:10.51271/JCCVS-0069

**Corresponding Author:** Gülhan Ayhan Albayrak, gulhanayhanalbayrak@gmail.com

**Received:** 14/01/2026

**Accepted:** 23/02/2026

**Published:** 28/03/2026

### ABSTRACT

**Aims:** Accurate risk stratification of pulmonary nodules incidentally detected during cardiovascular imaging is essential for guiding preoperative evaluation and cardiothoracic decision-making. This study aimed to identify independent predictors of pulmonary nodule malignancy and to develop a logistic regression-based risk scoring model, comparing its diagnostic performance with the Brock model.

**Methods:** This retrospective study included 125 patients with pulmonary nodules who underwent histopathological evaluation between January 2019 and December 2023. Patients were classified as benign (n=64) or malignant (n=61). Clinical characteristics and radiological parameters obtained from computed tomography and positron emission tomography/computed tomography were recorded. Univariable and multivariable logistic regression analyses were performed to identify independent predictors of malignancy. A weighted risk score was constructed based on regression coefficients. Discriminative performance was assessed using receiver operating characteristic curve analysis and compared with the Brock model using the DeLong test. A p value <0.05 was considered statistically significant.

**Results:** Multivariable analysis identified computed tomography nodule size, irregular margins, and pleural-based localization as independent predictors of malignancy (p<0.05). The proposed risk model demonstrated excellent discrimination with an area under the curve of 0.989 (95% confidence interval: 0.978–1.000), significantly superior to the Brock model (area under the curve=0.819; 95% confidence interval: 0.743–0.891; p<0.001). At the optimal cutoff value, sensitivity was 90.0% and specificity was 98.4%.

**Conclusion:** The developed logistic regression-based risk model provides a highly accurate tool for malignancy prediction in pulmonary nodules encountered during cardiovascular evaluation. Integration of this model into preoperative cardiovascular workflows may enhance multidisciplinary decision-making and reduce unnecessary invasive procedures.

**Keywords:** Risk assessment, cardiovascular imaging, thoracic surgery, neoplasm staging, diagnostic imaging

### INTRODUCTION

Incidental pulmonary nodules are frequently identified during thoracic imaging performed for cardiovascular evaluation and preoperative assessment. Accurate differentiation between benign and malignant nodules is critical in cardiothoracic practice, as inappropriate management may result in unnecessary surgical procedures or delayed oncologic intervention.<sup>1</sup> Pulmonary nodules are increasingly detected with the widespread use of thoracic computed tomography (CT), both in lung cancer screening programs and as incidental findings during imaging performed for other clinical indications. Meta-analyses conducted in recent years indicate that pulmonary nodules are identified in approximately one-quarter to one-third of chest CT examinations, the majority of which are benign; however, a clinically significant proportion represents malignant or premalignant lesions, highlighting the critical importance of accurate early characterization. Early and reliable differentiation between benign and malignant nodules is essential, as it directly influences clinical decision-making, patient outcomes, and healthcare resource

utilization. Although traditional radiological features—including nodule size, spiculated or irregular margins, and upper lobe location—remain important predictors of malignancy, reliance on individual imaging characteristics alone often provides insufficient diagnostic accuracy in routine clinical practice.<sup>1</sup>

Accurate differentiation between benign and malignant nodules is essential for guiding management decisions, including the need for surveillance imaging, positron emission tomography/computed tomography (PET/CT), or invasive diagnostics, and influences patient outcomes and healthcare utilization. Traditional CT morphological features—such as nodule size, margin characteristics (e.g., spiculation), density (solid vs subsolid), and lobar location—remain central to risk assessment in routine radiologic practice. However, individual radiological features alone often lack sufficient specificity and reproducibility to reliably distinguish malignant from benign nodules across diverse clinical contexts.<sup>2</sup>

CT-based radiomics has emerged as a noninvasive approach for more comprehensive characterization of pulmonary nodules beyond conventional visual assessment. Meta-analytic evidence demonstrates that radiomics-based models achieve high pooled diagnostic performance for malignancy prediction, with reported area under the curve (AUC) values of approximately 0.91, consistently outperforming traditional radiological evaluation in multiple studies.<sup>3,4</sup>

Furthermore, integration of radiomic features with epidemiological and clinical variables significantly enhances model discrimination, supporting the development of multimodal risk assessment frameworks. In parallel, PET/CT-based prediction models that combine metabolic activity with morphological parameters provide improved diagnostic accuracy compared with PET metrics alone, underscoring the added value of hybrid imaging approaches.<sup>5</sup> Nevertheless, substantial heterogeneity in study design, imaging protocols, and feature extraction methods highlights the need for standardized validation and model refinement. Additionally, the performance of established clinical prediction tools, such as the Brock model, demonstrates variable AUC values across different populations and nodule subtypes, reinforcing the necessity for external validation in diverse clinical cohorts.<sup>6</sup>

Recent advances in deep learning-based imaging analysis have shown promise in pulmonary nodule risk stratification. Approaches employing convolutional neural networks have demonstrated superior classification performance compared with traditional multiparametric statistical models across different clinical subgroups, supporting their potential role in enhancing diagnostic accuracy and facilitating integration into clinical workflows. However, challenges related to model generalizability, external validation, and interpretability remain significant barriers to widespread clinical implementation.<sup>7</sup>

Several prediction models have been proposed to estimate malignancy risk in pulmonary nodules, including the Brock model; however, their performance may vary across different populations and clinical settings. A comprehensive evaluation of clinical and radiological predictors, together with the development of practical risk scoring systems, may enhance individualized risk assessment and help reduce unnecessary invasive procedures.<sup>8</sup> Therefore, this study aimed to identify independent clinical and radiological determinants of pulmonary nodule malignancy, to develop a novel logistic regression-based risk scoring model applicable in cardiovascular clinical practice, and to compare its diagnostic performance with the established Brock model.

## METHODS

### Ethics

This study has been approved by the Ethics Committee of Şişli Hamidiye Etfal Training and Research Hospital (Date: 29.11.2022, Decision number: 2195). All procedures were carried out in accordance with the ethical rules and the principles of the Declaration of Helsinki.

### Study Design and Population

This retrospective cohort study included 125 consecutive adult patients ( $\geq 18$  years) with pulmonary nodules who underwent

histopathological evaluation between January 2021 and December 2022 at a tertiary care center with cardiovascular and cardiothoracic services. Patients with at least one pulmonary nodule detected on thoracic CT were eligible for inclusion. Inclusion criteria required the availability of diagnostic-quality thoracic CT imaging and definitive histopathological confirmation. Patients with incomplete clinical data, inadequate imaging quality, or inconclusive pathology results were excluded. Based on histopathological findings, patients were classified into two groups: benign nodules (n=64) and malignant nodules (n=61).

All eligible patients who met the predefined inclusion and exclusion criteria during the study period were included consecutively to minimize potential selection bias. Only patients with histopathologically confirmed diagnoses were analyzed to ensure diagnostic accuracy and avoid outcome misclassification. Patients whose pulmonary nodules were managed solely with radiological surveillance without tissue confirmation were not included in the final analysis.

The logistic regression model was developed using the entire study cohort. Due to the relatively limited sample size, no formal internal validation procedure (such as bootstrapping or split-sample validation) was performed. Therefore, the reported performance metrics reflect apparent model performance within the derivation dataset.

### Data Collection

Demographic and clinical data, including age, sex, smoking history, and family history of lung cancer, were obtained retrospectively from electronic medical records. Radiological characteristics were recorded from thoracic CT and PET/CT images.

### Radiological Evaluation

All CT and PET/CT examinations were reviewed by experienced thoracic radiologists blinded to the histopathological outcomes. Recorded radiological variables included nodule size, density (solid or part-solid), margin characteristics (regular or irregular), presence of air bronchogram, calcification, cavitation, pleural-based location, upper lobe localization, number of nodules (single vs. multiple), presence of emphysema, and maximum standardized uptake value (SUVmax) on PET/CT. An SUVmax value  $>2.5$  was considered positive for increased metabolic activity. Pulmonary nodules were evaluated in accordance with current international guidelines, and when multiple nodules were present, the most suspicious or largest nodule was selected for analysis.

All CT and PET-CT images were reviewed by a single board-certified thoracic radiologist with substantial experience in thoracic imaging. The radiologist was aware of the clinical indication but blinded to the final histopathological diagnosis at the time of imaging evaluation. No independent second reading or formal interobserver agreement analysis was performed.

### Brock Model Calculation

For each patient, the probability of malignancy was calculated using the Brock (Pan-Canadian Early Detection of Lung Cancer) model based on its original variables and coefficients. Brock scores were expressed as percentages and used for comparative performance analysis.

### Statistical Analysis

The data analyses were performed using IBM Statistical Package for the Social Sciences (SPSS) for macOS, version 30.0 (IBM Corp., Armonk, NY, USA). The distribution of continuous variables was assessed using the Kolmogorov–Smirnov test, histogram inspection, and evaluation of skewness and kurtosis values ( $\pm 2$ ). Categorical variables were presented as counts and percentages [n (%)]. Continuous variables were expressed as mean $\pm$ standard deviation for normally distributed data and as median (interquartile range, IQR) for non-normally distributed data. Comparisons between benign and malignant nodule groups were performed using Student’s t-test for normally distributed continuous variables and the Mann–Whitney U test for non-normally distributed continuous variables. Categorical variables were compared using the Pearson chi-square test or Fisher’s exact test, as appropriate.

Logistic regression analyses were conducted to identify factors associated with pulmonary nodule malignancy. Initially, univariate logistic regression analyses were performed for all variables. Variables with a p value <0.05 in univariate analysis, as well as those considered clinically relevant, were included in multivariate logistic regression analysis. Two separate logistic regression models were constructed.

Model A was designed to identify independent risk factors for malignancy by incorporating study-specific clinical and radiological variables. Based on the  $\beta$  coefficients obtained from the multivariate logistic regression analysis, a risk score model was developed to facilitate clinical applicability. Regression coefficients were scaled while preserving their relative magnitudes. Specifically, each  $\beta$  coefficient was divided by the smallest  $\beta$  coefficient in the model, and the resulting values were multiplied by 10 and rounded to the nearest integer to generate weighted scores. The total risk score was calculated by summing the individual scores for each variable, and individual malignancy probabilities were estimated using this total score. Model B was constructed using variables included in the Brock (Pan-Canadian Early Detection of Lung Cancer) model to evaluate the performance of the Brock model within the study population. Results of multivariate logistic regression analyses were reported as odds ratios (ORs) with 95% confidence intervals (CIs).

Predicted malignancy probabilities for Model A were obtained using the predicted probability outputs from the logistic regression analysis. Brock malignancy probabilities were calculated individually for each patient using the original coefficients defined in the PanCan model. The discriminative performance of the models was evaluated using ROC analysis, and the AUC was reported with 95% CIs. Differences between the AUCs of model A and the Brock model were compared using the DeLong method. A p value <0.05 was considered statistically significant for all analyses.

## RESULTS

Of the 125 patients included in the study, 64 (51.2%) had benign nodules and 61 (48.8%) had malignant nodules. The mean age of patients in the malignant group was significantly higher than that of the benign group (66 $\pm$ 13 vs. 59 $\pm$ 15 years, p=0.011). No statistically significant differences were

observed between the groups in terms of sex distribution or smoking history (p>0.05). From a radiological perspective, the presence of an air bronchogram was significantly more frequent in benign nodules (p=0.041). Malignant nodules were significantly larger in size on CT imaging compared with benign nodules (22.6 $\pm$ 4.9 mm vs. 17.9 $\pm$ 5.1 mm, p<0.001). In addition, CT attenuation values were significantly higher in malignant nodules than in benign nodules (p<0.001). Calcification was significantly more common in benign nodules (p<0.001). In contrast, pleural-based location, upper lobe localization, and irregular margin characteristics were observed significantly more frequently in malignant nodules (p<0.05). On PET/CT imaging, nodules with SUVmax >2.5 were significantly more prevalent in the malignant group (p<0.001). Furthermore, the Brock malignancy score was significantly higher in malignant nodules compared with benign nodules (44.0 $\pm$ 17.3 vs. 23.4 $\pm$ 13.5, p<0.001) (Table 1).

**Table 1.** Distribution of clinical, demographic, and radiological characteristics of patients with pulmonary nodules

Variables	Total	Benign (n=64)	Malignant (n=61)	p value
<b>Sex</b>				0.112
Male	73 (58.4)	33 (51.6)	40 (65.6)	
Female	52 (41.6)	31 (48.4)	21 (34.4)	
Age (years)	62 $\pm$ 15	59 $\pm$ 15	66 $\pm$ 13	0.011
Smoking history (smoker)	74 (59.2)	35 (54.7)	39 (63.9)	0.293
Air bronchogram	67 (53.6)	40 (62.5)	27 (44.3)	0.041
CT size (mm)	20.2 $\pm$ 5.5	17.9 $\pm$ 5.1	22.6 $\pm$ 4.9	<0.001
CT density (HU)	39 (24–70)	31.5 (16.5–43)	63 (37–86)	<0.001
Family history of lung cancer	24 (19.2)	15 (23.4)	9 (14.8)	0.218
<b>Number of nodules</b>				0.571
Single nodule	83 (66.4)	41 (64.1)	42 (68.9)	
Multiple nodules	42 (33.6)	23 (35.9)	19 (31.1)	
Calcification	35 (28.0)	1 (1.6)	34 (55.7)	<0.001
Cavitation	26 (20.8)	9 (14.1)	17 (27.9)	0.057
<b>Pleural location</b>				<0.001
Pleural-based	61 (48.8)	6 (9.4)	55 (90.2)	
Non-pleural-based	64 (51.2)	58 (90.6)	6 (9.8)	
Upper lobe location	40 (32.3)	13 (20.3)	27 (45.0)	0.003
Emphysema	26 (21.0)	12 (18.8)	14 (23.3)	0.531
<b>Margin characteristics</b>				<0.001
Smooth	57 (45.6)	51 (79.7)	6 (9.8)	
Irregular	68 (54.4)	13 (20.3)	55 (90.2)	
<b>PET SUVmax</b>				<0.001
Negative	65 (52.0)	51 (79.7)	14 (23.0)	
>2.5	60 (48)	13 (20.3)	47 (77)	
<b>Nodule type</b>				<0.001
Solid	85 (68)	28 (43.8)	57 (93.4)	
Part-solid	40 (32)	36 (56.3)	4 (6.6)	
Brock score (%)	33.4 $\pm$ 18.6	23.4 $\pm$ 13.5	44 $\pm$ 17.3	<0.001

Data are presented as number and percentage [n (%)] for categorical variables and as mean $\pm$ standard deviation or median (interquartile range, IQR) for continuous variables. CT: Computed tomography, HU: Hounsfield unit, PET: Positron emission tomography, SUVmax: Maximum standardized uptake value

In univariate analysis, age, CT nodule size, PET SUVmax >2.5, irregular margin characteristics, pleural-based location, and upper lobe localization were significantly associated with malignancy (p<0.05). In multivariate logistic regression analysis, CT nodule size (OR=1.236, 95% CI: 1.015-1.504; p=0.035), irregular margin characteristics (OR=90.005, 95% CI: 7.236-1119.562; p<0.001), and pleural-based location (OR=111.605, 95% CI: 10.683-1165.88; p<0.001) remained independent predictors of malignancy. Age and upper lobe localization lost statistical significance after adjustment for other variables (Table 2).

Based on the variables found to be independently associated with malignancy in multivariate analysis (model A), a final weighted risk score model was developed (Table 3). Regression coefficients were transformed into weighted scores to facilitate clinical applicability, and total scores ranged 0 to 32.

The linear predictor (LP) equation was defined as: LP=-6.896+0.380×(total score). As the total score increased, the estimated probability of pulmonary nodule malignancy increased markedly. The estimated probabilities of malignancy were derived from the underlying logistic regression model and subsequently mapped to predefined total score intervals (0-4: <5%; 5-9: 10-25%; 10-14: 25-50%; 15-19: 50-75%; ≥20: ≥85%). These probability thresholds were established to provide a clinically interpretable framework for risk stratification and management decision-making (Table 4).

In univariate analysis, age, CT nodule size, upper lobe localization, and irregular margin characteristics were significantly associated with malignancy (p<0.05) (Table 5). However, in multivariate analysis, only CT nodule size and irregular margin characteristics remained independent predictors of malignancy (p<0.001). Sex, family history of lung cancer, presence of emphysema, and number of nodules were not independently associated with malignancy (p>0.05).

The proposed model demonstrated excellent discriminative performance for predicting pulmonary nodule malignancy,

**Table 3.** Predictor variables and weighted scoring system derived from the multivariable logistic regression model

Variable	Criteria	Points
Age	+1 point per 10-year increase	1
Nodule size (CT)	+1 point per 5 mm increase	1
PET SUVmax ≥2.5	Yes	4
Irregular margin	Yes	12
Pleural-based localization	Yes	12
Upper lobe location	Yes	2
Total score range		0-32

CT: Computed tomography, PET: Positron emission tomography, SUVmax: Maximum standardized uptake value. Total score was calculated by summing the weighted points assigned to each predictor variable.

**Table 4.** Total score-based risk stratification and corresponding malignancy probabilities

Total score	Estimated probability of malignancy
0-4	<5%
5-9	10-25%
10-14	25-50%
15-19	50-75%
≥20	≥85%

The estimated probabilities of malignancy were derived from the underlying logistic regression model and subsequently mapped to predefined total score intervals (0-4: <5%; 5-9: 10-25%; 10-14: 25-50%; 15-19: 50-75%; ≥20: ≥85%). These probability thresholds were established to provide a clinically interpretable framework for risk stratification and management decision-making.

with an AUC of 0.989 (95% CI: 0.978-1.000; p<0.001). In contrast, the Brock model showed a lower discriminative performance, with an AUC of 0.819 (95% CI: 0.743-0.891; p<0.001). The difference between the two models was statistically significant (p<0.001) (Table 6, Figure). The sensitivity and specificity of the proposed model were 90.0% and 98.4%, respectively, whereas the Brock model demonstrated a sensitivity of 65.6% and a specificity of 87.5%.

Internal validation was performed using both split-sample (70% training, 30% testing) and bootstrap resampling

**Table 2.** Univariate and multivariate logistic regression analysis of factors associated with pulmonary nodule malignancy (model A)

Variables	Univariate analysis		Multivariate analysis	
	OR (95% CI)	p value	OR (95% CI)	p value
Age (years)	1.033 (1.007-1.060)	0.014	1.039 (0.974-1.108)	0.242
CT size (mm)	1.192 (1.104-1.288)	<0.001	1.236 (1.015-1.504)	0.035
<b>PET SUVmax</b>				
Negative	Reference	-	Reference	-
>2.5	13.170 (5.615-30.894)	<0.001	5.341 (0.872-32.712)	0.070
<b>Margin characteristics</b>				
Smooth	Reference	-	Reference	-
Irregular	35.962 (12.715-101.709)	<0.001	90.005 (7.236-1119.562)	<0.001
<b>Pleural location</b>				
Non-pleural-based	Reference	-	Reference	-
Pleural-based	88.611 (26.952-291.329)	<0.001	111.605 (10.683-1165.880)	<0.001
<b>Upper lobe location</b>				
No	Reference	-	Reference	-
Yes	3.210 (1.452-7.097)	0.004	1.964 (0.299-12.909)	0.482

Odds ratios (ORs) with 95% confidence intervals (CIs) were estimated using logistic regression analysis. Variables with p<0.10 in univariate analysis were entered into the multivariate model (model A). p-value <0.05 was considered statistically significant. CT: Computed tomography, PET: Positron emission tomography, SUVmax: Maximum standardized uptake value

**Table 5.** Logistic regression analysis of factors predicting pulmonary nodule malignancy according to the Brock model variables (model B)

Variables	Univariate analysis		Multivariate analysis	
	OR (95% CI)	p value	OR (95% CI)	p value
Age (years)	1.033 (1.007–1.060)	0.014	1.031 (0.991–1.072)	0.135
CT size (mm)	1.192 (1.104–1.288)	<0.001	1.252 (1.100–1.425)	<0.001
<b>Sex</b>				
Male	Reference	–	Reference	–
Female	0.559 (0.272–1.149)	0.114	1.753 (0.465–6.605)	0.407
<b>Upper lobe location</b>				
No	Reference	–	Reference	–
Yes	3.210 (1.452–7.097)	0.004	4.395 (0.653–29.580)	0.128
<b>Margin characteristics</b>				
Regular	Reference	–	Reference	–
Irregular	35.962 (12.715–101.709)	<0.001	79.399 (16.038–393.079)	<0.001
<b>Family history of lung cancer</b>				
No	Reference	–	Reference	–
Yes	0.565 (0.227–1.410)	0.221	0.525 (0.106–2.594)	0.429
<b>Emphysema</b>				
No	Reference	–	Reference	–
Yes	1.319 (0.554–3.139)	0.532	0.263 (0.058–1.183)	0.082
<b>Number of nodules</b>				
Single nodule	Reference	–	Reference	–
Multiple nodules	0.806 (0.383–1.698)	0.571	0.310 (0.053–1.812)	0.194

Odds ratios (ORs) and 95% confidence intervals (CIs) were calculated using logistic regression analysis. Reference categories are indicated. A p value < 0.05 was considered statistically significant. CT: Computed tomography

**Table 6.** ROC analysis results of the proposed model and the Brock model for predicting pulmonary nodule malignancy

Model	AUC (95% CI)	p value	Sensitivity (%)	Specificity (%)
Brock model	0.819 (0.743–0.891)	<0.001	65.6	87.5
Proposed logistic regression model	0.989 (0.978–1.000)	<0.001	90.0	98.4

AUC indicates area under the receiver operating characteristic (ROC) curve; AUC: Area under the curve, CI: Confidence interval. Sensitivity and specificity were calculated at the optimal cut-off values determined by ROC analysis. The diagnostic performance of the proposed model and the Brock model was evaluated using ROC curve analysis.

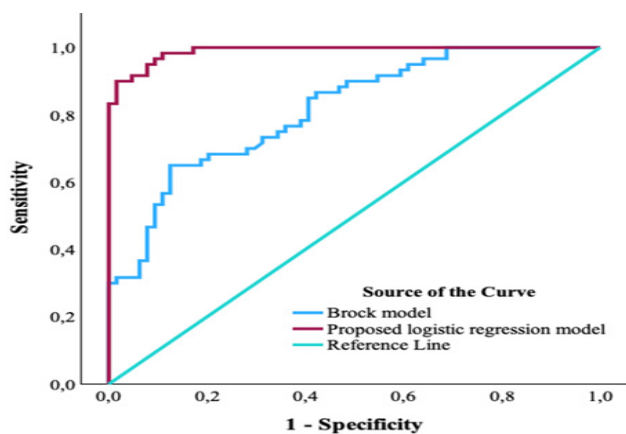


**Figure.** Comparison of ROC curves of the proposed logistic regression model and the Brock model for predicting pulmonary nodule malignancy  
ROC: Receiver operating characteristic

(1000 iterations). The model demonstrated consistently high discriminative performance in the development cohort (AUC=0.989). In split-sample validation, the AUC remained high (0.972). The optimism-corrected AUC after bootstrap was 0.983, indicating minimal overfitting. Nevertheless, external validation in an independent cohort is required before clinical implementation (Table 7).

**Table 7.** Internal validation and optimism-corrected performance of model A

Performance measure	AUC
Development cohort (entire dataset)	0.989
Split-sample validation (70% training–30% testing)	0.972
Optimism-corrected AUC (bootstrap, 1000 resamples)	0.983

Internal validation included split-sample (70/30) and bootstrap (1000 iterations) analyses. The optimism-corrected AUC (0.983) indicated minimal overfitting and good model stability. AUC: Area under the curve

## DISCUSSION

In this retrospective study, we developed a clinically applicable logistic regression–based risk model to predict pulmonary nodule malignancy and compared its diagnostic performance with the Brock model within a cardiovascular clinical context. The proposed model demonstrated excellent discriminative ability, significantly outperforming the Brock model, with an AUC of 0.989 versus 0.819. Our findings indicate that specific radiological characteristics—particularly nodule size, margin irregularity, and pleural-based localization—are strong independent predictors of malignancy.

Accurate risk stratification is especially important in patients undergoing cardiovascular evaluation and cardiothoracic surgical assessment, as incidentally detected pulmonary nodules may influence surgical planning, timing of intervention, and perioperative management strategies. Inadequate assessment may lead either to unnecessary invasive thoracic procedures or to delays in appropriate oncologic referral. The integration of a validated and practical risk scoring model into cardiovascular preoperative workflows may therefore enhance multidisciplinary decision-making, optimize patient selection for invasive procedures, and improve overall clinical management.

The high discriminative performance observed in this study may reflect the inclusion of strong radiological predictors such as nodule size, irregular margins, and pleural-based location. Nodule size remains one of the most robust predictors of malignancy in pulmonary nodules. In our study, malignant nodules were significantly larger than benign nodules, and nodule size remained an independent risk factor in multivariate analysis. This finding is consistent with current international guidelines and prior studies, which emphasize increasing malignancy risk with increasing nodule diameter.<sup>9,10</sup> Similarly, large population-based studies have demonstrated that nodule growth and size are key determinants in malignancy risk stratification.<sup>11</sup>

Margin characteristics emerged as one of the strongest predictors in our model. Irregular or spiculated margins were significantly more frequent in malignant nodules and demonstrated a very high OR in multivariate analysis. Irregular margins reflect invasive tumor growth and desmoplastic reaction and have been consistently associated with malignancy in prior radiological and pathological studies.<sup>9-12</sup> Our results reinforce the central role of detailed morphologic assessment in pulmonary nodule evaluation.

Pleural-based localization was another independent predictor of malignancy in our cohort. Malignant nodules were significantly more likely to be pleural-based compared with benign lesions. This finding may be related to the propensity of certain lung cancers, particularly adenocarcinomas, to arise in peripheral lung regions adjacent to the pleura.<sup>10,11</sup> Previous imaging studies have also highlighted pleural contact as a feature associated with increased malignancy risk.<sup>10</sup>

Functional imaging with PET/CT provided additional discriminatory value. Nodules with SUVmax values greater than 2.5 were significantly more frequent in the malignant group, consistent with previous reports demonstrating increased glucose metabolism in malignant pulmonary lesions.<sup>11</sup> From a practical clinical perspective, patients classified as low risk may be managed with structured radiological follow-up, intermediate-risk patients may benefit from further functional imaging such as PET/CT, whereas high-risk patients should be considered for prompt invasive diagnostic evaluation or surgical referral.

Beyond its diagnostic accuracy, the proposed risk score may have particular relevance in cardiovascular surgery and preoperative assessment settings, where incidental pulmonary nodules are frequently detected during routine

thoracic imaging. In such scenarios, accurate malignancy risk stratification is essential to optimize perioperative planning, avoid unnecessary delays in cardiac or vascular procedures, and prevent unwarranted invasive interventions. By providing a structured and quantitative risk estimate, the model may support multidisciplinary decision-making and contribute to safer and more individualized preoperative management strategies.

Although PET SUVmax demonstrated a strong association with malignancy in univariate analysis, it did not remain independently significant in the multivariable model. This finding may be explained by shared predictive information with other structural radiological variables, particularly nodule size and morphological characteristics, which are closely related to metabolic activity. In diagnostic cohorts enriched with clinically suspicious nodules, the incremental predictive contribution of SUVmax may diminish once strong anatomical predictors are included in the model. Importantly, the lack of independent statistical significance does not imply absence of clinical value; rather, it suggests that metabolic information provided by PET may partially overlap with morphological risk features captured by CT-based variables.<sup>12,13</sup>

Upper lobe localization was significantly associated with malignancy in univariate analysis but lost statistical significance after adjustment for other variables. This observation aligns with prior studies suggesting that upper lobe predominance is associated with lung cancer risk, particularly in smokers, but may be confounded by other radiological features when multivariate models are applied.<sup>14,15</sup>

The Brock model, originally developed in a low-risk lung cancer screening population, demonstrated lower discriminative performance in our cohort. This result was expected, as our study population consisted of patients with clinically suspicious nodules who underwent histopathological evaluation, rather than asymptomatic individuals detected through screening programs.<sup>16,17</sup> Screening-based models may underestimate malignancy risk when applied to higher-risk diagnostic populations.<sup>16,18</sup>

Although the proposed model demonstrated excellent discriminative performance with a high AUC value (0.989), this result should be interpreted with caution. The single-center design and relatively limited sample size may increase the risk of sample-specific overfitting. To mitigate this concern, internal validation using bootstrap resampling was performed, which supported the stability and robustness of the model estimates. Nevertheless, despite favorable internal validation results, external validation in independent and multicenter cohorts is essential to confirm the generalizability and reproducibility of the model across diverse patient populations before routine clinical implementation. Similar observations have been reported in diagnostic cohort-based prediction models.<sup>17</sup>

The proposed scoring system provides a transparent and quantitative framework for malignancy risk estimation that can be readily implemented in daily clinical workflow. Each predictor identified in the multivariable model is assigned

a weighted score proportional to its regression coefficient, allowing straightforward bedside calculation. Age contributes 1 point per 10-year increase, CT size contributes 1 point per 5-mm increase, PET SUVmax  $\geq 2.5$  adds 4 points, upper lobe location adds 2 points, while irregular margins and pleural-based localization—being the strongest predictors—contribute 12 points each. The total score ranges from 0 to 32 and is incorporated into the logistic equation ( $LP = -6.896 + 0.380 \times \text{total score}$ ) to derive the estimated probability of malignancy.

For clinical usability, total scores were stratified into actionable risk categories: 0–4 (<5% risk), 5–9 (10–25%), 10–14 (25–50%), 15–19 (50–75%), and  $\geq 20$  ( $\geq 85\%$  risk). This categorization enables immediate risk-adapted management decisions. For example, a patient accumulating  $\geq 20$  points—corresponding to an estimated malignancy probability of  $\geq 85\%$ —can be confidently prioritized for early invasive diagnostic procedures and cardiothoracic surgical evaluation, supported by the model's high specificity (98.4%). Conversely, patients with scores  $\leq 4$  (<5% risk) may be safely managed with structured radiological surveillance. By translating multivariable regression output into an intuitive point-based system with clearly defined probability thresholds, the model bridges statistical prediction and real-world clinical decision-making.

The observed performance differences between the proposed model and the Brock model should be interpreted in the context of underlying population characteristics. The Brock model was developed in a lung cancer screening cohort, where disease prevalence is relatively low and nodules are often smaller and incidentally detected.<sup>18</sup> In contrast, the present study was conducted in a diagnostic cohort enriched with histopathologically confirmed cases, resulting in a higher pretest probability of malignancy and a broader representation of clinically suspicious nodules. Such differences in case-mix, prevalence, and spectrum of disease are well known to influence model discrimination and calibration. Models developed in screening populations may exhibit attenuated performance when applied to diagnostic cohorts, and vice versa, highlighting issues of model transportability. Therefore, the superior discriminative performance observed in our cohort likely reflects both tailored predictor selection and the specific clinical context in which the model was derived. External validation in diverse clinical settings, including screening populations, will be essential to assess generalizability and transportability.<sup>19,20</sup>

Accurate preoperative assessment is a cornerstone of cardiothoracic surgical planning. Previous studies have demonstrated that inadequate risk stratification may increase perioperative morbidity and delay appropriate oncologic treatment.<sup>21–23</sup> In this context, integrating a validated radiological risk score into cardiovascular surgical workflows may improve patient selection and optimize perioperative outcomes.

### Limitations

Several limitations should be acknowledged. First, the retrospective and single-center design may limit the external validity and generalizability of the findings. Although consecutive patient inclusion was applied to reduce

selection bias, the study population consisted exclusively of histopathologically confirmed cases. Patients managed conservatively with radiological follow-up were not included, which may restrict applicability to lower-risk nodules encountered in routine screening or incidental detection settings. Therefore, a degree of selection bias cannot be entirely excluded.

Second, the relatively limited sample size and absence of internal validation procedures, such as bootstrapping or split-sample validation, should be considered when interpreting the excellent discriminative performance of the model (AUC=0.989). Although the high AUC likely reflects the use of histopathology as a reference standard, the clinically selected diagnostic cohort, and the inclusion of radiological variables with strong effect sizes—particularly irregular margins and pleural-based localization—the possibility of optimism bias or overfitting cannot be completely excluded.

Third, radiological assessments were performed by a single experienced thoracic radiologist. While this ensured consistency in image interpretation, interobserver variability was not evaluated. Consequently, the reproducibility of radiological feature assessment across different observers remains uncertain.

Taken together, these factors underscore the need for prospective, multicenter studies with larger and more heterogeneous populations, as well as formal internal and external validation, to confirm the robustness, calibration, transportability, and clinical utility of the proposed risk model.

## CONCLUSION

As a result, this study demonstrates that CT nodule size, irregular margin characteristics, and pleural-based localization are strong and independent predictors of pulmonary nodule malignancy. The proposed CT-based logistic regression-derived weighted risk score model showed superior diagnostic performance compared with the Brock model. Implementation of this practical and tailored prediction tool in cardiovascular and cardiothoracic clinical practice may enhance multidisciplinary decision-making, improve diagnostic accuracy, reduce unnecessary invasive procedures, and optimize perioperative patient management.

## ETHICAL DECLARATIONS

### Ethics Committee Approval

This study has been approved by the Ethics Committee of Şişli Hamidiye Etfal Training and Research Hospital (Date: 29.11.2022, Decision number: 2195).

### Informed Consent

As this was a retrospective study, formal written informed consent was not required and was therefore not obtained.

### Peer Review Process

This manuscript was subject to external peer review.

### Conflict of Interest

The author declare no conflicts of interest related to this study.

## Financial Disclosure

The author received no financial support for the conduct or publication of this research.

## Author Contributions

The author is solely responsible for the conception, design, data collection, analysis, interpretation, and writing of the manuscript.

## REFERENCES

- Chen D, Yang L, Zhang W, et al. Prevalence and management of pulmonary nodules: a systematic review and meta-analysis. *J Thorac Dis.* 2024;16(7):4619-4632. doi:10.21037/jtd-24-874
- MacMahon H, Naidich DP, Goo JM, et al. Guidelines for management of incidental pulmonary nodules detected on CT images: 2017 Fleischner Society guidelines. *Radiology.* 2017;284(1):228-243. doi:10.1148/radiol.2017161659
- Callister MEJ, Baldwin DR, Akram AR, et al. British Thoracic Society guidelines for the investigation and management of pulmonary nodules. *Thorax.* 2015;70(Suppl 2):ii1-ii54. doi:10.1136/thoraxjnl-2015-207168
- McWilliams A, Tammemägi MC, Mayo JR, et al. Probability of cancer in pulmonary nodules detected on first screening CT. *N Engl J Med.* 2013;369(10):910-919. doi:10.1056/NEJMoa1214726
- Ten Haaf K, van Rosmalen J, de Koning HJ, et al. External validation of lung cancer risk prediction models: a systematic review. *Thorax.* 2017;72(9):837-845. doi:10.1136/thoraxjnl-2016-208706
- Ten Haaf K, Jeon J, Tammemägi MC, et al. Risk prediction models for lung cancer screening. *JAMA.* 2020;323(7):1-11. doi:10.1001/jama.2019.22287
- Park S, Lee SM, Kim S, et al. Development and validation of a CT-based prediction model for pulmonary nodule malignancy. *Eur Respir J.* 2022;60(2):2102023. doi:10.1183/13993003.02023-2021
- Huang Y, Liu Z, He L, et al. Radiomics signature: a potential biomarker for the prediction of lung cancer malignancy in pulmonary nodules. *Eur Radiol.* 2020;30(5):2911-2921. doi:10.1007/s00330-019-06513-0.
- Wang H, Zhou Z, Li Y, et al. CT-based radiomics predicts the malignancy of pulmonary nodules: a systematic review and meta-analysis. *Acad Radiol.* 2023;30(12):3064-3075. doi:10.1016/j.acra.2023.05.012.
- Mu W, Jiang L, Zhang J, et al. Non-invasive decision support for lung cancer diagnosis based on PET/CT radiomics. *Eur J Nucl Med Mol Imaging.* 2020;47(3):635-644. doi:10.1007/s00259-019-04553-6
- Nam JG, Park S, Hwang EJ, et al. Development and validation of deep learning-based automatic detection algorithm for malignant pulmonary nodules on chest CT. *Radiology.* 2021;299(1):218-228. doi:10.1148/radiol.2021203846
- de Margerie-Mellon C, Onken A, Heidinger BH, et al. Pulmonary nodules: risk stratification using volumetric and morphologic CT features. *Radiology.* 2021;301(1):192-202. doi:10.1148/radiol.2021203981
- Truong MT, Sabloff BS, Ko JP. Multimodality imaging in the evaluation of pulmonary nodules. *Radiol Clin North Am.* 2020;58(1):41-58. doi:10.1016/j.rcl.2019.09.004
- Lowe VJ, Fletcher JW, Gobar L, et al. Prospective investigation of PET in lung nodules. *J Clin Oncol.* 2020;38(15 Suppl):e20532. doi:10.1200/JCO.2020.38.15\_suppl.e20532
- Horeweg N, Scholten ET, de Jong PA, et al. Detection of lung cancer through low-dose CT screening. *N Engl J Med.* 2020;382:503-513. doi:10.1056/NEJMoa1911793
- Baldwin DR, Gustafson J, Pickup L, et al. External validation of a radiological risk model for pulmonary nodules. *Thorax.* 2021;76(6):610-617. doi:10.1136/thoraxjnl-2020-215654
- Mazzone PJ, Lam L. Evaluating pulmonary nodules: clinical practice consensus guidelines. *Chest.* 2022;161(1):406-421. doi:10.1016/j.chest.2021.07.055
- Kim H, Lee SM, Seo JB, et al. External validation and comparison of the Brock model and Lung-RADS in a lung cancer screening cohort: results from the Cancer Screening Project. *Eur Radiol.* 2021;31(6):4004-4015. doi:10.1007/s00330-020-07567-9
- Li H, Salehjahromi M, Godoy MCB, et al. Lung cancer risk prediction in patients with persistent pulmonary nodules using the Brock model and Sybil model. *Cancers (Basel).* 2025;17(9):1499. doi:10.3390/cancers17091499
- Dinnessen R, Peeters D, Antonissen N, et al. Performance of a screening-trained deep learning model for pulmonary nodule malignancy estimation of incidental clinical nodules. *Eur Radiol.* 2026;36(1):85-95. doi:10.1007/s00330-025-11829-1
- Yang CJ, Kumar A, Deng JZ, et al. A national analysis of perioperative outcomes after lung cancer surgery. *Ann Thorac Surg.* 2021;111(4):1130-1138. doi:10.1016/j.athoracsur.2020.08.056
- Burt BM, Shrager JB. Incidental pulmonary nodules in patients undergoing cardiac surgery: clinical implications and management strategies. *Ann Thorac Surg.* 2022;113(5):1582-1589. doi:10.1016/j.athoracsur.2021.09.021
- Bilgin SS, Bilgin M. Radiological evaluation of pulmonary nodules. In: Soysal O, ed. *Approach to Pulmonary Nodules.* 1<sup>st</sup> ed. Türkiye Klinikleri; 2019.
- de Koning HJ, Meza R, Plevritis SK, et al. External validation of lung cancer risk prediction models: a systematic review. *Thorax.* 2017;72(9):837-845. doi:10.1136/thoraxjnl-2016-208964

## Should the postoperative ACT value be higher or lower than the preoperative value in cardiac surgery?

Osman Fehmi Beyazal\*, Mehmed Yanartaş

Department of Cardiovascular Surgery, Başakşehir Çam and Sakura City Hospital, İstanbul, Türkiye

Cite this article: Beyazal OF, Yanartaş M. Should the postoperative ACT value be higher or lower than the preoperative value in cardiac surgery? *J Cardiol Cardiovasc Surg.* 2026;4(1):14-20. doi:10.51271/JCCVS-0070

\*Corresponding Author: Osman Fehmi Beyazal, osmanfehmi beyazal@gmail.com

Received: 09/02/2026

Accepted: 26/03/2026

Published: 28/03/2026

### ABSTRACT

**Aims:** The aim of this study was to compare the activated clotting time (ACT) values after heparin neutralization with the values before heparin in patients undergoing cardiac surgery and to investigate the relationship with postoperative outcomes.

**Methods:** Between 2022 and 2023, a total of 726 patients (518 males; mean age 58.2±11.5 years) who underwent cardiac surgery were evaluated. The patients were initially divided into two groups. Group A (n=401): Patients whose ACT values before heparinization were lower than the ACT values after neutralization, and group B (n=325): Patients whose ACT values before heparinization were equal to or higher than the ACT values after neutralization.

**Results:** There were no differences between the groups in terms of bleeding amount and blood product use. However, the need for postoperative exploration and subxiphoid decompression was higher in group B than in group A (p=0.001 and p=0.008, respectively). Hospital stay did not differ between the groups. Intubation time and intensive care unit stay were longer in group B compared to group A (p=0.003 and p=0.04, respectively). Additionally, the mortality rate was higher in group B than in group A (p=0.02).

**Conclusion:** In cardiac surgery, we found no difference in bleeding amounts and blood product use between patients with post-neutralization ACT values higher than pre-heparin ACT values and those with lower ACT values. However, we observed higher postoperative exploration and mortality rates, as well as longer intubation times.

**Keywords:** Activated clotting time, heparin, protamine sulfate, cardiac surgery, bleeding

### INTRODUCTION

Cardiopulmonary bypass (CPB), first designed by John Gibbon in 1953, has enabled many cardiac operations to be performed successfully.<sup>1</sup> To use CPB, anticoagulation is often achieved using heparin, which is then neutralized with protamine sulfate. The anticoagulant activity of heparin is monitored using activated clotting time (ACT). Recommended ACT values range between 300 and 600 seconds, depending on the ACT measurement method.<sup>2</sup>

Bleeding and subsequent postoperative exploration after cardiac surgery are among the most important causes of morbidity and mortality. The overall incidence of exploration due to bleeding ranges between 2.3% and 6%.<sup>3</sup> One of the most important causes of bleeding is coagulopathy. Therefore, preoperative and postoperative ACT values are important in terms of bleeding. The appropriate protamine dose for heparin neutralization is a topic of debate. It is suggested that protamine should be given at a 1:1 ratio with heparin to minimize bleeding, and that this ratio should not be exceeded initially to avoid potential protamine overdose and increased perioperative bleeding.<sup>2</sup> In a prospective study by Taneja et al.,<sup>4</sup> it was reported that a protamine:heparin ratio of 0.3 was sufficient for some patients to neutralize

heparin, while a ratio of 0.5 was sufficient for most patients. It is also controversial what the ACT value should be after neutralization with protamine. In the study by Yamamoto et al.,<sup>5</sup> it was shown that there was no residual heparin in the blood after 1:1 protamine, but ACT values were longer, and clotting factors were lower. In the study by Wang et al.,<sup>6</sup> it was reported that postoperative ACT values shortened operative time, decreased bleeding, and reduced need for blood transfusion.

There are not enough studies to make a definitive decision on comparing the ACT values after neutralization with protamine with the ACT values before heparinization. The aim of this study was to compare the ACT values after heparin neutralization with the values before heparin in patients undergoing cardiac surgery and to investigate the relationship with postoperative outcomes.

### METHODS

This study has been approved by the Clinical Researches Ethics Committee of Başakşehir Çam and Sakura City Hospital (Date: 23.10.2023, Decision No: 2023-443). All

procedures were carried out in accordance with the ethical rules and the principles of the Declaration of Helsinki.

This study was designed as a retrospective single-center observational study with a total of 726 patients. All patients over the age of 18 who underwent cardiac surgery at the Cardiovascular Surgery Clinic of Başakşehir Çam and Sakura City Hospital between February 2022 and July 2023 were included in the study. Patients who underwent surgery due to aortic dissection and those who used extracorporeal membrane oxygenation or intraaortic balloon pumps in the perioperative period were excluded from the study. The patients were first divided into two groups. Group A (n=401): Patients whose ACT values before heparinization were lower than the ACT values after neutralization, and group B (n=325): Patients whose ACT values before heparinization were equal to or higher than the ACT values after neutralization.

All patients' basic demographic characteristics, medical history, preoperative and first-week postoperative laboratory parameters, surgical procedure details, and postoperative complications (postoperative exploration, subxiphoid decompression, cerebrovascular accident (CVA), continuous renal replacement therapy (CRRT), postoperative atrial fibrillation (POAF), deep sternal wound infection (DSWI), intubation time, intensive care unit stay, hospital stay and mortality) were recorded by reviewing their medical records. Then, preoperative and perioperative data and postoperative complications were compared between the groups. Afterward, patients who received dual antiplatelet therapy in the preoperative period were excluded from both groups. Subgroups were obtained as group C (n=325) and group D (n=269), respectively. In the second stage, group C and group D were compared in terms of postoperative parameters.

In our clinic, all patients who have undergone CABG are taken into surgery without stopping acetylsalicylic acid. For patients who have recently undergone percutaneous intervention, the decision of whether or not dual antiplatelet therapy will be continued is made by the primary surgeon, depending on the status of coronary artery lesions. Intravenous heparin (Poliparin, Polifarma, İstanbul, Türkiye) is administered to all patients who underwent cardiac surgery using CPB at a dose of 3 mg/kg to reach the target value of 480 sec ACT before starting CPB. ACT values are tested with Hemochron® Signature Elite (International Technidyne Corporation, Edison, NJ, USA). Preoperative ACT is tested after anesthesia induction. Following heparin administration, control ACT values are checked 3 minutes later, and then control values are checked every 30 minutes during CPB. Additional doses of heparin are administered when necessary. Protamine sulfate (Promin, Vem, Türkiye) is used for neutralization at a ratio of 1:1. After protamine, the ACT value is checked 5 minutes later. In patients with serious bleeding diathesis, if the ACT values are higher than the pre-heparin value after neutralization, additional protamine is administered.

### Statistical Analysis

Data were analyzed by using SPSS software version 27.0 (IBM, USA). Continuous variables in the study were presented as minimum, maximum, median, and interquartile range. Categorical variables were expressed as numbers and

percentages. The normality of distribution was assessed by the Kolmogorov–Smirnov test. For numerical variables, differences between patients and controls were tested using t test for parametric data or the Mann–Whitney U test for non-parametric data. Categorical variables were analyzed using the Pearson  $\chi^2$  test and Fisher's exact test. The level of statistical significance was set at  $p < 0.05$ .

## RESULTS

The comparison of patient demographics, comorbidities, and laboratory parameters between group A and group B is presented in **Table 1**. The mean age was  $58.2 \pm 11.5$  years and 518 (71.3%) of the patients were male. The mean follow-up period was  $245 \pm 126$  days, (median: 279, 0–535 days). There were no significant differences between groups A and B in terms of basic demographic characteristics, except for the median age values, which were higher in group B ( $p = 0.03$ ). Comorbidities showed no difference between the two groups. Additionally, there were no significant differences between group A and group B in terms of preoperative and postoperative 1st-week laboratory parameters, except for the median preoperative and postoperative creatinine values, which were higher in group B than in group A ( $p < 0.001$  and  $p = 0.004$ , respectively).

The comparison of operative data between group A and group B is presented in **Table 2**. No differences were found between the groups in terms of emergency operation rates and types of operations performed. Similarly, no differences were found between the groups in terms of cross-clamp (XCL) times and CPB times.

A comparison of blood product, bleeding data, and medication data between Group A and Group B is presented in **Table 3**. No differences were found between the groups in terms of intraoperative red blood cells (RBCs), fresh frozen plasma (FFP), and platelet suspension. Similarly, no differences were found in terms of postoperative RBCs and platelet suspension. Only in group B, postoperative FFP usage was more common than in group A ( $p = 0.01$ ). No difference was found between the groups in terms of postoperative bleeding amounts. The rates of being operated on under dual antiplatelet therapy were higher in group B than in group A ( $p = 0.01$ ). Preoperative and postoperative acetylsalicylic acid use, postoperative oral anticoagulant use, and postoperative dual antiplatelet use were also similar between the groups. Preoperative median ACT values of group A were higher than in group B (150 sec and 124 sec, respectively,  $p < 0.001$ ). After the operation, the median ACT values of group A were lower than group B (123 sec and 143 sec, respectively,  $p < 0.001$ ). No difference was found between group A and group B in terms of heparin, protamine sulfate, and fibrinogen doses used during the operation. Higher doses of tranexamic acid were used in group B compared to group A ( $p = 0.03$ ).

The comparison of postoperative data between group A and group B is presented in **Table 4**. There was no difference between the groups in terms of the incidence of CVA, CRRT, POAF, and DSWI. The need for postoperative exploration and subxiphoid decompression was higher in group B than in group A (46 (%14.2) vs. 27 (%6.7),  $p = 0.001$  and 8 (%2.5)

**Table 1.** Comparison of patient demographics, comorbidities, and laboratory parameters between group A and group B

	Group A (n=401)			Group B (n=325)			p
	Min-max or n (%)	Median	IQR	Min-max or n (%)	Median	IQR	
<b>Demographic data</b>							
Gender male	298 (74.3)			220 (67.7)			0.05
Age (years)	19-86	59	14	18-90	60	14	0.03
Height (cm)	142-196	169	54	140-190	169	12	0.33
Weight (kg)	42-130	78	20	39-150	80	19	0.39
Body surface area (kg/m <sup>2</sup> )	1.33-2.42	1.89	0.24	1.22-2.6	1.89	0.23	0.90
Body-mass index (m <sup>2</sup> )	15.9-55.6	27.6	6.6	15.6-46.2	27.8	6.4	0.04
<b>Comorbid diseases</b>							
Diabetes mellitus	159 (39.7)			126 (38.8)			0.80
Hypertension	199 (49.6)			170 (52.3)			0.47
Chronic obstructive pulmonary disease	36 (9)			31 (9.5)			0.79
Cerebrovascular accident	29 (7.2)			33 (10.2)			0.16
Chronic renal failure	15 (3.7)			19 (5.8)			0.18
Malignancy	20 (5)			14 (4.3)			0.66
Ejection fraction (%)	22-65	60	10	15-65	55	10	0.39
Preop atrial fibrillation	30 (7.5)			29 (8.9)			0.48
<b>Preop laboratory parameters</b>							
White blood cells (10 <sup>9</sup> /L)	1.9-19.9	8.1	3	3.5-92	8.1	3	0.74
Hematocrit (%)	22-51.9	40.6	6.8	20.5-58.7	40	7.8	0.44
Platelets (10 <sup>9</sup> /L)	63-563	235	87	59-688	250	102.5	0.39
Urea (mg/dl)	7.8-272	33.4	15.9	13.8-138	35.2	18.5	0.01
Creatinine (mg/dl)	0.07-10.9	0.90	0.27	0.48-5.4	0.96	0.3	<0.001
Sodium (mEq/L)	122-147	139	4	120-149	139	4	0.74
Potassium (mEq/L)	2.2-5.9	4.3	0.56	3.2-5.8	4.4	0.59	0.29
Alanine aminotransferase (IU/L)	1-301	18	13	3-338	18	12	0.85
Aspartate aminotransferase (IU/L)	4-431	20	10	9-321	20	10.5	0.87
C-reactive protein (mg/dl)	0.2-195	3.8	7.5	1-162	3.7	9.2	0.79
Hba1c (mmol/mol)	2.9-13.5	6	1.5	4.4-14.3	5.9	1.3	0.057
<b>Postop laboratory parameters</b>							
White blood cells (10 <sup>9</sup> /L)	4.6-44.2	16.1	8.3	5.2-72	16	8.7	0.99
Hematocrit (%)	12.9-46.5	28.7	5.7	14-47.1	28.5	5.8	0.56
Platelets (10 <sup>9</sup> /L)	32.9-480	169	79.5	48-496	175	86	0.36
Urea (mg/dl)	13.5-200	41.3	18	14.5-129	41.3	18.9	0.68
Creatinine (mg/dl)	0.08-7.8	1.18	0.42	0.49-6.1	1.24	0.49	0.004
Sodium (mEq/L)	126-163	142	4	133-163	142	4	0.42
Potassium (mEq/L)	2.9-8.9	4.2	0.59	2.6-5.7	4.1	0.78	0.13
Alanine aminotransferase (IU/L)	4-302	23	18	2-850	22	17	0.58
Aspartate aminotransferase (IU/L)	13-912	59	41.5	8-2512	61	45	0.87
C-reactive protein (mg/dl)	2.9-315	38.4	28.3	4.6-276	36.4	25.7	0.13

Min: Minimum, Max: Maximum, IQR: Interquartile range

vs. 1 (0.2),  $p=0.008$ , respectively). There was no difference between the groups in terms of hospital stay. However, the intubation time and intensive care unit (ICU) stay were longer in group B than in group A (median 12 hours vs. 10 hours,  $p=0.003$ , 3 days, and 2 days,  $p=0.04$ , respectively). The mortality rate was higher in group B than in group A (32 (9.8%) and 22 (5.5%), respectively,  $p=0.02$ ).

After excluding patients who underwent surgery without stopping dual antiplatelet drugs, the remaining patients in

both groups were compared based on postoperative data, as presented in **Table 5**. There were no differences between group C and group D in terms of CVA, POAF, DSWI, ICU stay, and hospital stay. However, the need for postoperative exploration and subxiphoid decompression was higher in group D compared to group C (36 (13.4%) vs. 22 (6.8%), respectively,  $p=0.007$ , and 7 (2.6%) vs. 1 (0.3%),  $p=0.01$ ). Additionally, intubation time and mortality rate were longer in group D than in group C ( $p=0.004$  and  $p=0.04$ , respectively).

**Table 2.** Comparison of operative data between group A and group B

	Group A (n=401)			Group B (n=325)			p
	Min-max or n (%)	Median	IQR	Min-max or n (%)	Median	IQR	
Emergency surgery	18 (4.5)			16 (4.9)			0.78
Infective endocarditis	16 (4)			11 (3.4)			0.66
Thoracic surgery	26 (6.5)			28 (8.6)			0.27
Aortic valve replacement	77 (19.2)			65 (20)			0.78
Aortic root enlargement	3 (0.7)			4 (1.2)			0.38
Mitral valve replacement	65 (16.2)			57 (17.5)			0.63
Mitral ring annuloplasty	11 (2.7)			10 (3.1)			0.79
Tricuspid valve replacement	8 (2)			8 (2.5)			0.67
Tricuspid ring annuloplasty	22 (5.5)			18 (5.5)			0.97
Pulmonary valve replacement	3 (0.7)			0			0.16
Ablation	13 (3.2)			9 (2.7)			0.71
Atrial septal defect	23 (5.7)			14 (4.3)			0.38
Morrow	0			3 (0.9)			0.08
Coronary artery bypass graft	269 (67.1)			211 (64.9)			0.54
Beating heart	14 (3.5)			17 (5.2)			0.24
Endarterectomy	12 (3)			7 (2.2)			0.48
The number of grafts	0-7	2	3	0-5	2	3	0.44
Left ventricular assist device	2 (0.5)			4 (1.2)			0.25
Commando procedure	1 (0.2)			1 (0.3)			0.69
Redo	28 (7)			18 (5.5)			0.42
Cross-clamp time (minute)	0-321	87	64	0-323	90	66	0.48
Cardiopulmonary bypass time (minute)	0-444	135	64	0-515	136	71	0.39

Min: Minimum, Max: Maximum, IQR: Interquartile range

**Table 3.** Comparison of blood product, bleeding data and medication data between group A and group B

	Group A (n=401)			Group B (n=325)			p
	Min-max or n (%)	Median	IQR	Min-max or n (%)	Median	IQR	
<b>Blood product and bleeding data</b>							
Intraop RBC using	0-10	0	2	0-7	0	2	0.38
Intraop FFP using	0-4	0	0	0-4	0	0	0.33
Intraop platelet suspensions	0-6	0	0	0-6	0	0	0.16
Postop RBC using	0-13	0	1	0-24	0	2	0.055
Postop FFP using	0-12	0	1	0-9	0	2	0.01
Postop platelet suspensions	0-5	0	0	0-9	0	0	0.06
Postop 1 <sup>st</sup> day amount of bleeding (ml)	50-4200	400	290	50-3000	400	300	0.37
Postop 2 <sup>nd</sup> day amount of bleeding (ml)	0-1700	250	240	0-2200	250	250	0.75
<b>Preop medication data</b>							
Preop acetylsalicylic acid	288 (71.8)			226 (69.5)			0.50
Operation without stopping dual antiplatelet therapy	5 (1.2)			14 (4.3)			0.01
Postop oral anticoagulant	143 (35.6)			130 (40)			0.23
Postop acetylsalicylic acid	299 (74.5)			246 (75.6)			0.72
Postop dual antiplatelet	199 (49.6)			143 (44)			0.13
<b>Intraop medication data</b>							
Preop ACT (second)	101-357	150	36	56-201	124	25	<0.001
Dose of heparin administered (IU)	5000-50000	30000	5000	5000-65000	30000	5000	0.40
Dose of protamine administered (IU)	0-50000	30000	5000	0-60000	30000	5000	0.44
ACT after protamine (second)	57-228	123	23	89-339	143	29	<0.001
Dose of tranexamic acid (mg)	0-3000	1000	1500	0-6000	1000	1500	0.03
Dose of fibrinogen concentrate (mg)	0-4000	0	1000	0-4000	0	1000	0.56

Min: Minimum, Max: Maximum, IQR: Interquartile range, ACT: Activated clotting time, RBC: Red blood cells, FFP: Fresh frozen plasma, Intraop: Intraoperative, Postop: Postoperative, Preop: Preoperative

**Table 4.** Comparison of postoperative data between group A and group B

	Group A (n=401)			Group B (n=325)			p
	Min-max or n (%)	Median	IQR	Min-max or n (%)	Median	IQR	
Postop exploration	27 (6.7)			46 (14.2)			0.001
Subxiphoid decompression	1 (0.2)			8 (2.5)			0.008
Cerebrovascular accident	8 (2)			3 (0.9)			0.19
Continuous renal replacement therapy	20 (5)			9 (2.8)			0.12
Postop atrial fibrillation	92 (22.9)			82 (25.2)			0.47
Deep sternal wound infection	8 (2)			12 (3.7)			0.16
Intubation time (hour)	1-1145	10	8	2-672	12	8	0.003
Intensive care unit stay (days)	1-120	2	1	1-28	3	2	0.04
Hospital stay (days)	1-124	7	4	1-111	7	5	0.38
Mortality	22 (5.5)			32 (9.8)			0.02

Min: Minimum, Max: Maximum, IQR: Interquartile range

**Table 5.** Comparison of postoperative data between group C and group D

	Group C (n=325)			Group D (n=269)			p
	Min-max or n (%)	Median	IQR	Min-max or n (%)	Median	IQR	
Postoperative exploration	22 (6.8)			36 (13.4)			0.007
Subxiphoid decompression	1 (0.3)			7 (2.6)			0.01
Cerebrovascular accident	7 (2.2)			3 (1.1)			0.25
Continuous renal replacement therapy	18 (5.5)			5 (1.9)			0.02
Postop atrial fibrillation	79 (24.3)			68 (25.3)			0.78
Deep sternal wound infection	6 (1.8)			10 (3.7)			0.16
Intubation time (hour)	1-1145	10	9	2-672	11	8	0.004
Intensive care unit stay (days)	1-120	2	1	1-28	3	2	0.09
Hospital stay (days)	1-120	7	4	1-111	7	5	0.50
Mortality	19 (5.8)			27 (10)			0.04

Min: Minimum, Max: Maximum, IQR: Interquartile range

## DISCUSSION

Despite numerous advancements, such as advanced technology, modern equipment, and surgical techniques that do not require stopping the heart, CPB is still commonly utilized in cardiac surgery today. One of the major challenges associated with CPB is the need for effective anticoagulation. Unfractionated heparin is considered the gold standard for anticoagulation during CPB due to its quick onset of action, reliability, and rapid reversal with protamine sulfate.<sup>7</sup> However, even if neutralization is achieved, postoperative bleeding continues to be a significant cause of morbidity and mortality due to many factors, such as the high bleeding risk of cardiac surgery, factors related to the operation, and coagulopathy caused by CPB.<sup>8</sup> One way to prevent this is to completely neutralize the anticoagulant effect of heparin. The dosage of protamine sulfate used for this purpose has not been determined.<sup>2,4,9,10</sup> While the dose of protamine sulfate that should be administered is important, another important point is the target ACT value. After the heparin dose is compensated, additional protamine administration may cause protamine overdose and consequent bleeding.<sup>11</sup> Therefore, it is important to obtain the ACT value after the planned dose of protamine sulfate has been administered. This ACT value may be below, above, or similar to the preoperative value. There is no definitive consensus on how much this value should be reduced after the operation. High postoperative

ACT values (especially ACT  $\geq 140$  sec) are associated with an increased risk of bleeding and transfusion.<sup>12</sup> However, due to the risk of increased bleeding due to protamine overdose, the target ACT value is not certain. Therefore, in this study, we aimed to investigate the relationship between postoperative complications and whether the postoperative ACT value was reduced below the preoperative ACT value.

There are many risk factors for postoperative bleeding, such as patient factors, comorbid diseases, medications used, operation type, CPB, and XCL times. However, the most important point in our study is that the basic characteristics of the patient groups are similar. We did not detect any significant differences in terms of basic demographic characteristics, comorbid diseases, laboratory parameters, operation type and types, XCL and CPB times, and medications used. The most important difference between the groups is the rate of being taken to surgery under dual antiplatelet therapy. This was found to be higher in group B than in group A. Therefore, to eliminate the effect of this risk factor, these patients were excluded from the study and subgroups were obtained as group C and group D, and the comparison was made again in terms of postoperative results. However, in both comparisons between the groups, in the groups where postoperative ACT values were above preoperative values, postoperative exploration, need for subxiphoid decompression, and mortality rates were higher,

and the intubation time was longer. In the study by Wang et al.,<sup>6</sup> it was reported that lower postoperative ACT values than ACT values before heparin administration were associated with lower operative time, bleeding, and blood transfusion. However, this study was conducted only on CABG patients and with relatively fewer patients (n=398) than our study. Zahid et al.<sup>13</sup> reported similar intraoperative and postoperative results in a study comparing 101 patients whose ACT values were within and outside 10% of the initial value after protamine. One of the important points of our study is that it was conducted with a larger number of patients compared to similar studies on this subject and included other types of operations in cardiac surgery. Despite a complicated patient group and the high number of concomitant procedures, probably due to the larger number of patients, the basic characteristics and types of operations were similar between the groups. Moreover, CPB and XCL times, among the most important risk factors for bleeding, were also similar between the groups.

We did not find any difference in intraoperative blood product usage between group A and group B. There were no differences in postoperative RBCs and platelet suspension, while only FFP usage was higher in group B compared to group A. Interestingly, we did not find any difference in postoperative bleeding amounts between group A and group B. However, the need for postoperative exploration was higher in group B and group D. While the median ACT after neutralization was 123 sec in group A, it was 143 sec in group B. The higher postoperative exploration rates in group B may be related to the higher ACT value compared to group A. Indeed, it has been shown that an ACT value >140 sec is associated with bleeding, which supports this result.<sup>12</sup> However, considering that the postoperative bleeding amounts are similar, it would not be correct to say that ACT is the only reason for this. Considering that the need for postoperative exploration and subxiphoid decompression can occur at any time after the operation and that the median follow-up period of our study was 245±126 days, other factors than early ACT elevation also play a role in this. Heparin rebound may be an important factor in this. Heparin rebound has been defined as the return of heparin to circulation in the postoperative period despite apparently sufficient neutralization with protamine.<sup>14</sup> According to one review, the incidence of heparin rebound in cardiac surgery is approximately 40%.<sup>15</sup> Such a frequent occurrence may have increased the need for postoperative exploration in the group that already had higher ACT values. However, as we mentioned in the limitations of our study, we could not compare ACT values during postoperative follow-up hours between the groups. It would be useful to investigate this in future studies.

Another point to consider is the comparison of the drugs used. Preoperative and postoperative acetylsalicylic acid use, postoperative oral anticoagulant use, and postoperative dual antiplatelet use were similar between groups A and B. Even though there was no significant difference in the early postoperative period, the efficacy levels of the drugs may have differed, especially in discharged patients, due to irregular oral anticoagulant use. The data regarding the international normalized ratio (INR) follow-up between the groups could not be compared. In addition, bleeding may occur due to the procoagulant effect after overdose of protamine sulfate.

However, there was no difference in the doses of heparin and protamine sulfate administered between the groups.

We did not find any difference between the groups in terms of CVA, CRRT, POAF, and DSWI. In addition, we did not find any difference in the length of hospital stay between all groups. ICU time and intubation time were longer in group B than in group A. Intubation time was longer in group D than in group C. We think that these were due to more postoperative exploration, as expected. Similarly, the mortality rate was higher, probably due to more exploration. These results support that postoperative ACT values above the preoperative values are associated with higher bleeding-related adverse events, morbidity, and mortality than those below. However, future studies are needed to give a definitive idea about how much ACT should be reduced. It is also essential to avoid unnecessary protamine use due to the procoagulant effect of excessive protamine sulfate. Prolonged ACT, poor clot structure, and platelet dysfunction occur, especially with protamine administration at a ratio greater than 1:1.3.<sup>16</sup> In addition, hypotension, pulmonary vasoconstriction, allergic reactions, pulmonary hypertension, bronchoconstriction, and anaphylactic reactions may develop with protamine administration.<sup>17</sup> Therefore, caution should be exercised when administering additional doses of protamine, the target ACT value should be carefully determined, and most importantly, the patient should be carefully evaluated in terms of bleeding risk. In patients who are considered to have a high risk of bleeding during surgery, administering an additional dose of protamine sulfate to keep the target ACT value below 140 will be beneficial in reducing bleeding-related complications.

### Limitations

The most important limitation of the study is that it is retrospective. Secondly, ACT values were measured only as a single value preoperatively, intraoperatively, and postoperatively. ACT values in the following hours could not be accessed and therefore this analysis could not be performed. Frequently seen conditions such as heparin rebound could not be evaluated for this reason. Thirdly, the patient group was heterogeneous. Only isolated CABG patients were not included. A data group including complex patients with multiple concomitant procedures was evaluated. Another point is that the drug types of patients receiving dual antiplatelet could not be separated. Drugs containing different active ingredients may have affected the results. Finally, data regarding INR monitoring in the postoperative period could not be evaluated, especially for patients receiving oral anticoagulants. In addition, in a very labile measurement method such as INR, sudden increases and decreases may be observed at any time during the follow-up period. It does not seem possible to evaluate this clearly.

### CONCLUSION

In cardiac surgery, we found no difference in bleeding amounts and blood product use in patients with post-neutralization ACT values higher than pre-heparin ACT values compared to patients with lower ACT values. However, we observed higher postoperative exploration and mortality rates and longer intubation times. Patients should be carefully evaluated for bleeding risk. In patients with high bleeding risk, additional doses of protamine sulfate, which will reduce

the target ACT value to 140 seconds, may reduce bleeding-related complications.

## ETHICAL DECLARATIONS

### Ethics Committee Approval

This study has been approved by the Clinical Researches Ethics Committee of Başakşehir Çam and Sakura City Hospital (Date: 23.10.2023, Decision No: 2023-443).

### Informed Consent

Written informed consent was obtained from all individual participants prior to their inclusion in the study. Participants were fully informed about the study's aims, procedures, potential risks and benefits, and their rights—including the right to withdraw at any time without consequence. All participants voluntarily signed a written informed consent form.

### Peer Review Process

This manuscript was subject to external peer review.

### Conflict of Interest

The authors declare no conflicts of interest related to this study.

### Financial Disclosure

The authors received no financial support for the conduct or publication of this research.

### Author Contributions

Concept: OFB; Design: OFB; Control: OFB; Resources: OFB; Materials: OFB; Data Collection and/or Processing: OFB; Analysis and/or Interpretation: OFB; Literature Review: OFB; Writing the Article: OFB, MY; Critical Review: OFB, MY.

## REFERENCES

- Edmunds LH Jr. The evolution of cardiopulmonary bypass: lessons to be learned. *Perfusion*. 2002;17(4):243-251. doi:10.1191/0267659102pf585oa
- Task Force on Patient Blood Management for Adult Cardiac Surgery of the European Association for Cardio-Thoracic Surgery (EACTS) and the European Association of Cardiothoracic Anaesthesiology (EACTA), Boer C, Meesters MI, et al. 2017 EACTS/EACTA Guidelines on patient blood management for adult cardiac surgery. *J Cardiothorac Vasc Anesth*. 2018;32(1):88-120. doi:10.1053/j.jvca.2017.06.026
- Elassal AA, Al-Ebrahim KE, Debis RS, et al. Re-exploration for bleeding after cardiac surgery: reevaluation of urgency and factors promoting low rate. *J Cardiothorac Surg*. 2021;16(1):166. doi:10.1186/s13019-021-01545-4
- Taneja R, Szoke DJ, Hynes Z, Jones PM. Minimum protamine dose required to neutralize heparin in cardiac surgery: a single-centre, prospective, observational cohort study. *Can J Anaesth*. 2023;70(2):219-227. doi:10.1007/s12630-022-02364-4
- Yamamoto T, Wolf HG, Sinzobahamvya N, Asfour B, Hraska V, Schindler E. Prolonged activated clotting time after protamine administration does not indicate residual heparinization after cardiopulmonary bypass in pediatric open heart surgery. *Thorac Cardiovasc Surg*. 2015;63(5):397-403. doi:10.1055/s-0035-1554998
- Wang W, Wang Y, Wang J, et al. ACT values after neutralization lower than pre-heparinization ACT leads to lower operative times, bleeding, and post-operative transfusions in CABG patients: an observational study. *Braz J Cardiovasc Surg*. 2018;33(6):588-596. doi:10.21470/1678-9741-2018-0116
- Boysan E, Circi R, Beyazal OF, Şener E. Bivalirudin for cardiopulmonary bypass in a patient with heparin allergy. *J Cardiothorac Surg*. 2023;18(1):258. doi:10.1186/s13019-023-02359-2
- Bartoszko J, Karkouti K. Managing the coagulopathy associated with cardiopulmonary bypass. *J Thromb Haemost*. 2021;19(3):617-632. doi:10.1111/jth.15195
- De Simone F, Nardelli P, Licheri M, et al. Less is more: we are administering too much protamine in cardiac surgery. *Ann Card Anaesth*. 2021;24(2):178-182. doi:10.4103/aca.ACA\_26\_19
- Murugesh WR, Prasad SS, Ramachandrapa Sujay K, Dinesh Kumar US. Is a fixed low-dose protamine better at reducing postoperative bleeding in off pump coronary artery bypass grafting? *Asian Cardiovasc Thorac Ann*. 2021;29(9):922-927. doi:10.1177/0218492321997393
- Boer C, Meesters MI, Veerhoek D, Vonk ABA. Anticoagulant and side-effects of protamine in cardiac surgery: a narrative review. *Br J Anaesth*. 2018;120(5):914-927. doi:10.1016/j.bja.2018.01.023
- Pereira RM, Magueijo D, Guerra NC, et al. Activated clotting time value as an independent predictor of postoperative bleeding and transfusion. *Interdiscip Cardiovasc Thorac Surg*. 2024;38(5):ivae092. doi:10.1093/icvts/ivae092
- Zahid MA, Ahmed SS, Yousuf MS, Wadho SA, Akhtar MI, Hamid M. Post-neutralisation activated clotting time and postoperative transfusions in cardiac surgery outcome. *J Coll Physicians Surg Pak*. 2024;34(11):1275-1280. doi:10.29271/jcpsp.2024.11.1280
- Stone ME, Vespe MW. Heparin rebound: an in-depth review. *J Cardiothorac Vasc Anesth*. 2023;37(4):601-612. doi:10.1053/j.jvca.2022.12.019
- Rijkema M, Vlot EA, Stehouwer MC, Bruins P. Does heparin rebound lead to postoperative blood loss in patients undergoing cardiac surgery with cardiopulmonary bypass? *Perfusion*. 2024;39(8):1491-1515. doi:10.1177/02676591231199218
- Slaughter TF, LeBleu TH, Douglas JM Jr, Leslie JB, Parker JK, Greenberg CS. Characterization of prothrombin activation during cardiac surgery by hemostatic molecular markers. *Anesthesiology*. 1994;80(3):520-526. doi:10.1097/00000542-199403000-00007
- Levy JH, Ghadimi K, Kizhakkedathu JN, Iba T. What's fishy about protamine? Clinical use, adverse reactions, and potential alternatives. *J Thromb Haemost*. 2023;21(7):1714-1723. doi:10.1016/j.jth.2023.04.005

## Repair of anomalous left circumflex dominant coronary artery originating from right pulmonary artery in an adult age patient: surgical correction with ligation and bypass graft: a case report

 Manpal Loona<sup>\*1</sup>,  Irfan Yacoob Bhatt<sup>2</sup>,  Pawan Malik<sup>3</sup>

<sup>1</sup>Department of Cardiothoracic and Vascular Surgery, Kailash Hospital, Uttrakhand, India

<sup>2</sup>Department of Interventional Cardiology, Kailash Hospital, Uttrakhand, India

<sup>3</sup>Department of Cardiac Anaesthesia and Critical Care, Kailash Hospital, Uttrakhand, India

**Cite this article:** Loona M, Bhatt IY, Malik P. Repair of anomalous left circumflex dominant coronary artery originating from right pulmonary artery in an adult age patient: surgical correction with ligation and bypass graft: a case report. *J Cardiol Cardiovasc Surg.* 2026;4(1):21-24. doi:10.51271/JCCVS-0071

\*Corresponding Author: Manpal Loona, dr.manpallona@gmail.com

Received: 11/12/2025

Accepted: 22/03/2026

Published: 28/03/2026

### ABSTRACT

Bland-White-Garland syndrome also known as anomalous origin of left coronary artery from pulmonary artery (ALCAPA) is a rare anomaly of coronary arteries among all congenital heart defects. Its clinical presentation at different age, either in children or adulthood has significant impact on outcomes leading to myocardial ischemia and heart failure. Early diagnosis of ALCAPA with the help of multislice CT angiography or detailed catheter study is always good for the patient to prevent the possible grave consequences. Surgical approach remains to be the definite treatment modality for ALCAPA with variable approaches and surgical methods to repair. We hereby present a case of 53 years male with ALCAPA from branched right pulmonary artery with collaterals between RCA and LCA.

**Keywords:** Anomalous coronary, ALCAPA, BWG syndrome

### INTRODUCTION

Among all congenital heart diseases, anomalous coronary artery originating from pulmonary artery has been documented as one of the rare anomaly, which is being encountered in almost 1 in 300,000 cases worldwide.<sup>1</sup> This anomaly was first clinically described in 1933 by Edward Bland, Paul Dudley White, and Joseph Garland, also known as Bland White Garland syndrome or anomalous left coronary origin from pulmonary artery (ALCAPA).<sup>2</sup> This anomalous coronary origin leads to ischemia in left coronary system which further leads to ventricular dysfunction, mitral regurgitation and sudden cardiac death. This anomaly has been subdivided into two subtypes: infant and adult with its presentation at different age depending upon ischemia tolerance and collateral formation with age. Trans-thoracic imaging modality with other non invasive investigations CT angiography and magnetic resonance angiography can be used to identify the abnormality. Aim of the treatment for such anomaly remains confined to reconstruction for two separate coronary systems. There are several techniques for surgical repair including coronary button transfer, trans-pulmonary baffle creation or flaps, and coronary artery bypass grafting with ostial ligation. While some patients may still experience symptoms after the operation, the majority of patients recovers with their left ventricular function and is no longer at risk of sudden death. Further, severity of clinical presentation depends on steal of blood from coronaries and age.<sup>2,3</sup>

We hereby present a rare case of anomalous partial left circumflex coronary originating from right pulmonary artery presenting in adulthood with mild to moderate heart failure features with successful surgical repair.

### CASE

A male patient aged 53 years, presented to our hospital in cardiology unit with chief complaints of dyspnoea with abrupt onset of on and off pain in chest radiating to neck. On evaluation his blood pressure was recorded 132/84 mm of Hg, SpO<sub>2</sub> 98% at room air, heart rate of 92 beats per minute. On further examination, his trans thoracic echocardiography revealed mild RV dilation with LVEF 45-48% (Simpson's method). Chest X ray was normal and ECG was found to be in sinus rhythm. Considering his clinical presentation with insignificant findings, detailed cardiac evaluation was planned. CT Coronary angiography was performed, which revealed anomalous coronary with its ostia originating from right pulmonary artery (RPA) along with separate two normal coronary ostia originating from aorta as usual on left and right coronary positions along with co-dominance of left and right coronaries (**Figure 1**). Considering ambivalent results of CT coronary angiogram, further evaluation based on standard coronary angiography with cardiac catheterization study was performed, which revealed two separate normal coronary ostia for right and left coronary arising from aorta

along with anomalous coronary connection between RPA and left circumflex coronary artery (LCX). It also revealed co-dominance of both left and right coronary system with significant collaterals connecting both sides (**Figure 2**). As per cardiac catheterization results, patient was planned for surgical intervention in view of persistent symptoms.

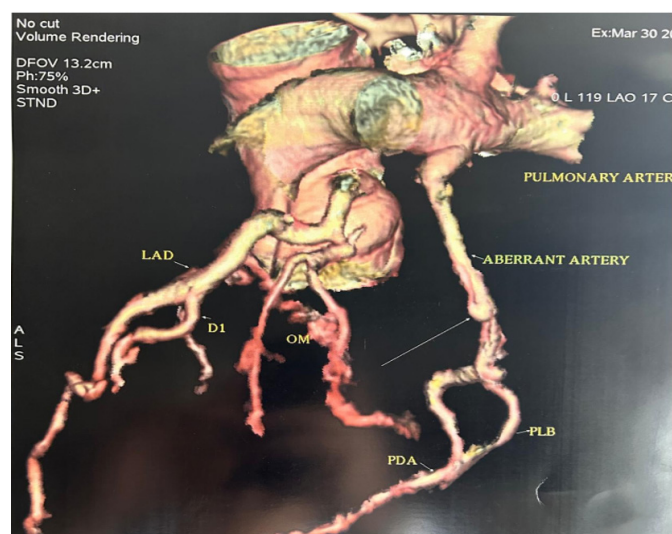


**Figure 1.** CT images of coronary angiogram showing anomalous coronary origin from right pulmonary artery  
CT: Computed tomography, PDA: Patent ductus arteriosus



**Figure 2.** Conventional images of coronary angiogram one catheter placed in main pulmonary artery from right atrium, while other catheter spilling contrast into left main ostia with its spillage further into right pulmonary artery through a separate origin of dominant left circumflex coronary artery co-dominant system with collaterals between left and right coronaries

### Surgical Procedure

Standard midline sternotomy was done. Aorto-bicaval cannulation was done. Cardiopulmonary bypass (CPB) was established with mild hypothermia of 32 degrees. RPA was dissected and anomalous connection was found between RPA and left circumflex coronary origin running behind aorta. Initial plan was to re-implant coronary ostia to aorta directly, considering the length of anomalous coronary was found short and tortuous course of coronary running behind aorta into posterior myocardium, plan of surgical repair from coronary re-implantation was converted to ostial ligation and bypass graft (**Figure 3**). Coronary ostial end was identified, looped around and snuggled for 5 minutes

and checked for any ECG changes. This depicted mild ECG changes with ST elevation of 0.06 mm in antero-lateral leads. Considering mild ECG changes, coronary artery bypass with one saphenous venous grafting was done for obtuse marginal vessel with proximal end anastomosed to aorta. Anomalous left circumflex coronary ostial connection originating from RPA was ligated juxta-pulmonary origin externally and clipped. CPB was weaned on minimal inotropic support. Total CPB time of 58 minutes with cross clamp time was 25 minutes. The postoperative course was uneventful, and patient was extubated on the first postoperative day. He was discharged on the fifth postoperative day. Patient is doing well with his 10 months follow up without any symptoms and preserved ejection fraction.

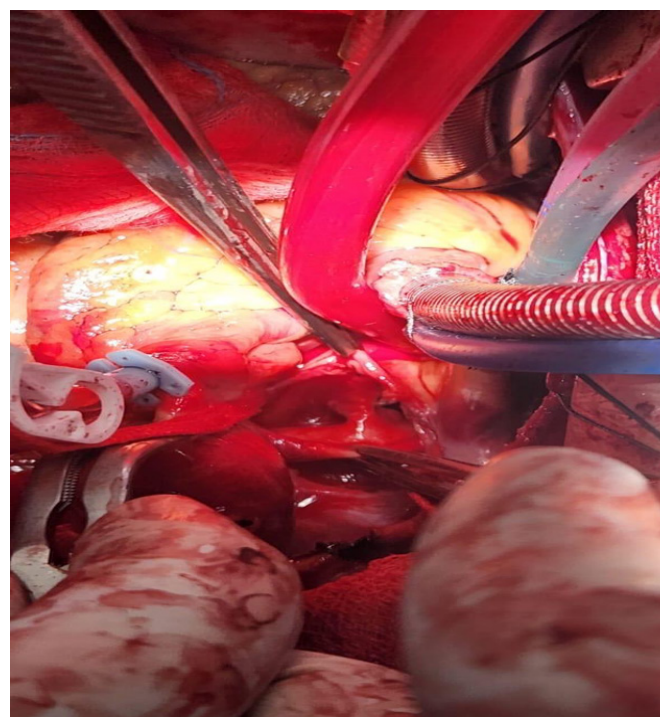


**Figure 3.** Intra-operative image depicting anomalous coronary ostia of dominant left circumflex originating from right pulmonary artery as shown in image between forceps holding tissue

### DISCUSSION

Based on presentation of age, ALCAPA patients are typically classified into two types depending on the presence of collaterals:

- The adult type for those with well-established collaterals and
- The infantile type for those without collaterals.

Certain factors such as the timing of the closure of the patent ductus arteriosus (PDA), the pressure gradient between the pulmonary and coronary arteries, and the development of collaterals, as well as the type of coronary anatomy plays a vital role in presenting symptoms of the patient.<sup>3,4</sup> Surgery is recommended in patients with ALCAPA, even in the absence of symptoms or a significant left-to-right shunt syndrome, given the risk of ventricular arrhythmias and sudden death.<sup>3</sup> Intracoronary collateral arteries benefit such patient for survival beyond infancy.<sup>5</sup> Multislice CT angiography plays pivotal role for non-invasive imaging with its spatial resolution for diagnosis of abnormal coronary arteries and their course.<sup>4,5</sup> Aim of surgical treatment for ALCAPA

patient remains confined to establish a two coronary vascular system to provide oxygenated blood to entire heart. Various surgical methods depending upon coronary origin from pulmonary trunk has been performed over the time and such surgical techniques are used depending upon variable anatomy, which includes direct re-implantation of coronary to aorta (coronary button transfer), intra-pulmonary baffle repair (the Takeuchi technique), subclavian coronary artery anastomosis and coronary artery bypass grafting with ostial ligation. Heart transplant remains reserved for the patient presenting late with poor ejection fraction.

It has been found in past by treating such patients may still experience symptoms after the operation, despite majority of patients recover left ventricular function and are no longer at risk of sudden death.<sup>6,7</sup> In a case series reported by Mishra et al.,<sup>8</sup> the outcomes of 105 patients with anomalous origin of the coronary artery from the pulmonary artery and 98 patients with ALCAPA; the median age at operation was 5.8 months with a median follow-up of 5.9 years. All patients underwent coronary re-implantation. In-hospital mortality was reported to be 8.5%, with no reported late deaths. In the Mishra series, 33.6% of patients who underwent surgery during the newborn period (<6 months of age) had good recovery of left ventricular function (mean left ventricular ejection fraction from 50 to 55%) and had improvement in mitral regurgitation from moderate severity to mild residual regurgitation. In addition, 52% of the patients who underwent operations late in infancy (after 6 months of age) had residual impairment of left ventricular function (mean left ventricular ejection fraction from 40 to 50%) and mild-to-moderate mitral regurgitation.<sup>8</sup>

Another review study of 98 infant ALCAPA cases, Radman et al.<sup>9</sup> found that approximately three years after corrective surgery, left ventricular function returned to normal in 98% of cases, whereas the trajectory of mitral regurgitation was more difficult to predict. The uncertainty regarding the improvement of mitral regurgitation was thought to be caused by potentially irreversible preoperative ischemia or suboptimal coronary perfusion after surgical correction due to loss of patency in the left coronary artery.<sup>9</sup>

The type of surgical correction being done, invariably impact the outcome and postoperative complications.

Surgical ligation when performed can lead to re-canalization and persistent silent ischemia with mitral regurgitation and may sometimes lead to sudden death.

Direct re-implantation technique when performed in infancy has good outcomes, but at the same when performed in adult age can lead to coronary artery tearing and bleeding, as it has decreased elasticity and high chance of kinking ostia during its mobilization.

Pulmonary baffle technique (Takeuchi repair) can lead to supra-valvular pulmonary artery obstruction, coronary-pulmonary fistula or aortic regurgitation.

Coronary artery bypass grafting in adult has been found to present promising results with internal mammary artery and saphenous vein graft with good calibre.<sup>8,10</sup>

Very few patients may present with residual symptoms due to irreversible myocardial damage and ischemia prior to surgery. At the same, a small subset of patients with poor ejection fraction may need implantable cardioverter defibrillators (ICD) in order to support left ventricle and dysarrhythmias in post operative period. Regular follow up is required in postoperative duration with monitored cardiac function, including ECG, echocardiogram and cardiac magnetic resonance imaging which help in long term outcomes.

Further survival of a patient depends on presenting illness along with factors such as age of presentation, lung maturity, the ratio of the left and right shunting, the development of collateral circulation, and the predominance of the right coronary artery and opting appropriate surgical method at correct time. Surgical treatment was chosen for our patient based on age, good collateral development and based on symptoms, ostial ligation with coronary graft was applied following this patient had uneventful outcome with early recovery.<sup>7,11</sup>

## CONCLUSION

We hereby conclude that considering every individual as separate entity with such cardiac anomaly, one should plan for patient looking at his diagnostic approach followed by appropriate method of surgery for survival benefit along with best outcomes for ALCAPA patients. Since over the past such anomaly has been found with anomalous origin of coronary arising from main pulmonary trunk but in our case it has been found arising from right branch of pulmonary trunk, which can be helpful for surgeons treating such condition in future. Such need of treatment plan helps not only patient but surgeon as well depending upon his best outcomes.

## ETHICAL DECLARATIONS

### Informed Consent

Written informed consent was obtained from the patient included in this report. Signed consent forms are retained by the authors and are available upon request.

### Peer Review Process

This report underwent external peer review.

### Conflict of Interest

The authors declare no conflicts of interest.

### Financial Disclosure

This case report did not receive any financial support.

### Author Contributions

Concept: ML, IYB, PM; Design: ML, IYB, PM; Control: ML, IYB, PM; Resources: ML, IYB, PM; Materials: ML, IYB, PM; Data Collection and/or Processing: ML, IYB, PM; Analysis and/or Interpretation: ML, IYB, PM; Literature Review: ML, IYB, PM; Writing the Article: ML, IYB, PM; Critical Review: ML, IYB, PM.

## REFERENCES

1. Dodge-Khatami A, Mavroudis C, Backer CL. Anomalous origin of the left coronary artery from the pulmonary artery: collective review of surgical therapy. *Ann Thorac Surg.* 2002;74(3):946-955. doi:10.1016/s0003-4975(02)03633-0

2. Sinha SK, Verma CM, Krishna V, et al. ALCAPA in an octogenarian woman: an enigma. *Cardiol Res.* 2015;6(3):289-291. doi:10.14740/cr400w
3. Boutsikou M, Shore D, Li W, et al. Anomalous left coronary artery from the pulmonary artery (ALCAPA) diagnosed in adulthood: varied clinical presentation, therapeutic approach and outcome. *Int J Cardiol.* 2018;261:49-53. doi:10.1016/j.ijcard.2018.02.082
4. Kerut EK, Kogos PG, Anderson JH, et al. Adult presentation of ALCAPA: echo and CT diagnosis. *Echocardiography.* 2018;35(7):1045-1048. doi:10.1111/echo.13807
5. Ajam A, Rahnamoun Z, Sahebjam M, et al. Cardiac imaging findings in anomalous origin of the coronary arteries from the pulmonary artery; narrative review of the literature. *Echo Res Pract.* 2022;9(1):12. doi:10.1186/s44156-022-00012-7
6. Hsu WF, Lee PC, Li HY, et al. Diagnosis and surgical outcomes of patients with anomalous left coronary artery from the pulmonary artery: a single Taiwanese Medical Center experience. *Heart Surg Forum.* 2020;23(2):E101-E106. doi:10.1532/hcf.2703
7. Dodge-Khatami A, Mavroudis C, Backer CL. Anomalous origin of the left coronary artery from the pulmonary artery: collective review of surgical therapy. *Ann Thorac Surg.* 2002;74(3):946-955. doi:10.1016/s0003-4975(02)03633-0
8. Mishra A. Surgical management of anomalous origin of coronary artery from pulmonary artery. *Indian J Thorac Cardiovasc Surg.* 2021;37(Suppl 1):131-143. doi:10.1007/s12055-021-01147-8
9. Radman M, Mastropietro CW, Costello JM, et al. Intermediate outcomes after repair of anomalous left coronary artery from the pulmonary artery. *Ann Thorac Surg.* 2021;112(4):1307-1315. doi:10.1016/j.athoracsur.2020.06.130
10. Peña E, Nguyen ET, Merchant N, Dennie C. ALCAPA syndrome: not just a pediatric disease. *Radiographics.* 2009;29(2):553-565. doi:10.1148/rg.292085059
11. Lange R, Vogt M, Hörer J, et al. Long-term results of repair of anomalous origin of the left coronary artery from the pulmonary artery. *Ann Thorac Surg.* 2007;83(4):1463-1471. doi:10.1016/j.athoracsur.2006.11.067

## Very late-onset pacemaker pocket infection presenting as a giant granulomatous mass

Öğuz Kağan Şentürk<sup>1</sup>, Berat Uğuz\*<sup>1</sup>, İsmet Zengin<sup>1</sup>, Tufan Günay<sup>1</sup>, İlken Uğuz<sup>2</sup>

<sup>1</sup>Department of Cardiology, Bursa City Hospital, Bursa, Türkiye

<sup>2</sup>Department of Anesthesiology and Reanimation, Bursa City Hospital, Bursa, Türkiye

Cite this article: Şentürk OK, Uğuz B, Zengin İ, Günay T, Uğuz İ. Very late-onset pacemaker pocket infection presenting as a giant granulomatous mass. *J Cardiol Cardiovasc Surg.* 2026;4(1):25-27. doi:10.51271/JCCVS-0072

\*Corresponding Author: Berat Uğuz, beratuguz33@hotmail.com

Received: 04/01/2026

Accepted: 25/03/2026

Published: 28/03/2026

### ABSTRACT

Pacemaker-related infections are most commonly observed during the early postoperative period; however, in rare instances, they may present many years after device implantation. We report an unusual case of a giant granulomatous pacemaker pocket infection occurring 10 years after the initial implantation. The patient presented with localized inflammatory signs without systemic manifestations. Following complete surgical removal of the device and the associated mass, histopathological examination confirmed xanthogranulomatous inflammation. *Staphylococcus epidermidis* was isolated from tissue cultures. Complete device extraction combined with prolonged antimicrobial therapy resulted in full clinical resolution, followed by successful contralateral reimplantation. This case highlights the importance of maintaining long-term vigilance in patients with cardiac implantable electronic devices.

**Keywords:** Pacemaker, pocket infection, xanthogranulomatous inflammation, cardiac implantable electronic device, late-onset infection

### INTRODUCTION

Permanent pacemaker implantation is a cornerstone therapy in the management of advanced atrioventricular conduction disorders and symptomatic bradyarrhythmias.<sup>1</sup> Although the majority of cardiac implantable electronic device (CIED)-related infections occur within the first year after implantation, late-onset infections presenting several years later are uncommon but clinically significant.<sup>2</sup> Such infections may manifest as localized generator pocket infections or progress to systemic endovascular involvement, frequently necessitating complete device and lead removal. We present a rare case of a giant granulomatous pacemaker pocket infection developing 10 years after implantation, emphasizing the importance of recognizing atypical and delayed presentations.

### CASE

A 78-year-old woman with a history of dual-chamber (DDDR) pacemaker implantation performed 10 years earlier for complete atrioventricular block was admitted with progressive swelling, erythema, and warmth over the left pectoral pacemaker pocket. She denied fever, chills, weight loss, or other constitutional symptoms. One year before presentation, she had noticed mild serous discharge from the implantation site, which resolved spontaneously without medical evaluation.

On physical examination, vital signs were stable, and there were no signs of systemic infection. Electrocardiography demonstrated a paced rhythm. Transthoracic echocardiography

revealed preserved left ventricular systolic function (ejection fraction 50%), mild-to-moderate mitral and tricuspid regurgitation, and no evidence of lead-associated vegetations. Soft tissue ultrasonography demonstrated a well-defined cystic lesion measuring approximately 12×7 cm overlying the generator pocket (Figure 1).

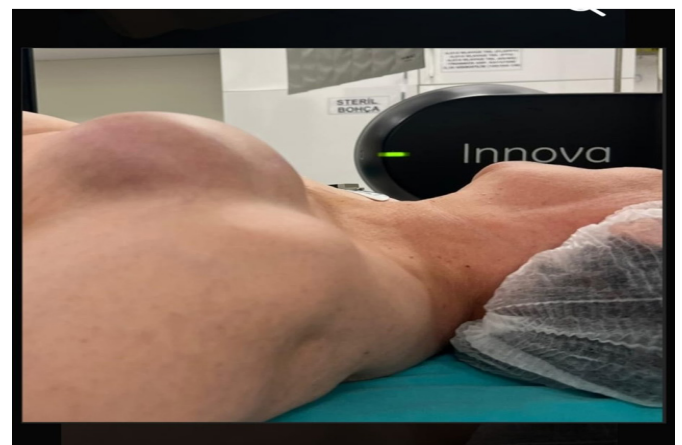


Figure 1. Preoperative external view of the left pectoral region showing prominent swelling over the pacemaker site

Given the high suspicion of a chronic pocket infection, the patient underwent complete device and lead extraction under sterile conditions. Intraoperatively, purulent material and extensive granulomatous tissue surrounding the generator and leads were identified (Figure 2). The encapsulated mass was excised in its entirety and submitted for histopathological

examination (**Figure 3**). Tissue cultures were obtained from the generator, leads, and pocket tissue. A temporary pacemaker was implanted, and empiric intravenous vancomycin and piperacillin–tazobactam therapy was initiated.



**Figure 2.** Granulomatous tissue excised from the pacemaker pocket during surgical exploration

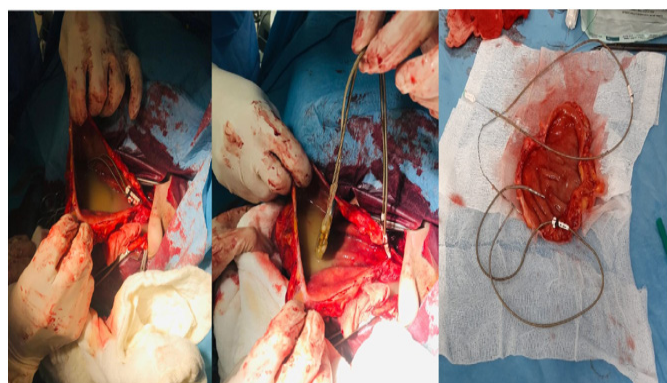


**Figure 3.** Intraoperative view showing pus accumulation and pacemaker leads within the pocket

Microbiological cultures yielded *Staphylococcus epidermidis*, and histopathological examination demonstrated chronic xanthogranulomatous inflammation characterized by lipid-laden macrophages and multinucleated giant cells.<sup>3</sup> Based on culture results, antimicrobial therapy was adjusted accordingly and continued for 14 days. Following completion of antibiotic treatment and confirmation of infection resolution, a new DDDR pacemaker system was successfully implanted in the contralateral subclavian region. The patient recovered uneventfully, with no evidence of recurrent infection during follow-up.

## DISCUSSION

Pacemaker pocket infections typically represent early postoperative complications; however, delayed presentations occurring years after implantation have been increasingly reported, particularly in aging device populations.<sup>2</sup> Late-onset infections may result from hematogenous seeding, local trauma, repeated microinjury to the pocket, or reactivation of dormant bacterial biofilms on device surfaces.<sup>4</sup> Biofilm formation on device surfaces plays a key role in delayed infections and contributes to antimicrobial resistance.

Xanthogranulomatous inflammation is a rare form of chronic inflammatory response characterized histologically

by lipid-laden macrophages, multinucleated giant cells, and fibrosis. Although most commonly described in the kidney and gallbladder, its occurrence in pacemaker pockets is exceptionally rare and may clinically mimic neoplastic or benign soft tissue masses, potentially delaying diagnosis.

*Staphylococcus epidermidis*, a common skin commensal organism, remains one of the most frequently isolated pathogens in CIED-related infections owing to its strong biofilm-forming capacity.<sup>3</sup> The cornerstone of management for established pacemaker pocket infections is complete removal of all hardware, including leads, followed by targeted antimicrobial therapy and delayed contralateral reimplantation. Conservative approaches without device extraction are associated with high relapse rates and are generally discouraged.

This case underscores the importance of maintaining a high index of suspicion for pacemaker pocket infections regardless of the time elapsed since implantation, even in the absence of systemic symptoms.

## CONCLUSION

Very late-onset pacemaker pocket infections are rare but clinically important entities that should be considered in patients presenting with localized inflammatory findings, even many years after device implantation. A multidisciplinary approach involving cardiology, electrophysiology, and infectious disease specialists is essential. Complete device extraction, appropriate antimicrobial therapy, and contralateral reimplantation can result in favorable clinical outcomes.

## ETHICAL DECLARATIONS

### Informed Consent

Written informed consent was obtained from the patient included in this report. Signed consent forms are retained by the authors and are available upon request.

### Peer Review Process

This report underwent external peer review.

### Conflict of Interest

The authors declare no conflicts of interest.

### Financial Disclosure

This case report did not receive any financial support.

### Author Contributions

Concept and Design: BU, OKŞ; Data Collection: BU, İZ, TG; Analysis and Interpretation of Data: İZ, TG; Drafting of the Manuscript: BU, İU, OKŞ; Final Approval of the Version to be Published: All Authors

## REFERENCES

1. Blomström-Lundqvist C, Auricchio A, Brugada J, et al. 2021 ESC guidelines on cardiac pacing and cardiac resynchronization therapy. *Eur Heart J*. 2021;42(35):3427-3520. doi:10.1093/eurheartj/ehab364
2. Baddour LM, Epstein AE, Erickson CC, et al. Update on cardiovascular implantable electronic device infections and their management: a scientific statement from the American Heart Association. *Circulation*. 2010;121(3):458-477. doi:10.1161/CIRCULATIONAHA.109.192665

- 
- 
3. Sohail MR, Uslan DZ, Khan AH, et al. Management and outcome of permanent pacemaker and implantable cardioverter-defibrillator infections. *J Am Coll Cardiol.* 2007;49(18):1851-1859. doi:10.1016/j.jacc.2007.01.072
  4. Tarakji KG, Chan EJ, Cantillon DJ, et al. Cardiac implantable electronic device infections: presentation, management, and patient outcomes. *Heart Rhythm.* 2010;7(8):1043-1047. doi:10.1016/j.hrthm.2010.05.016